Electronic Supplementary Material (ESI) for ChemComm.

Supporting Information

A Modular Design for Minor Groove Binding and Recognition of Mixed Base Pair Sequences of DNA

Pu Guo, Ananya Paul, Arvind Kumar, Narinder K. Harika, Siming Wang, Abdelbasset A. Farahat, David W. Boykin, W. David Wilson*

Department of Chemistry and Center for Diagnostics and Therapeutics, Georgia State University, Atlanta, GA 30303-3083 (USA)

Table of Contents

General Materials and Methods

Synthesis

Scheme S1

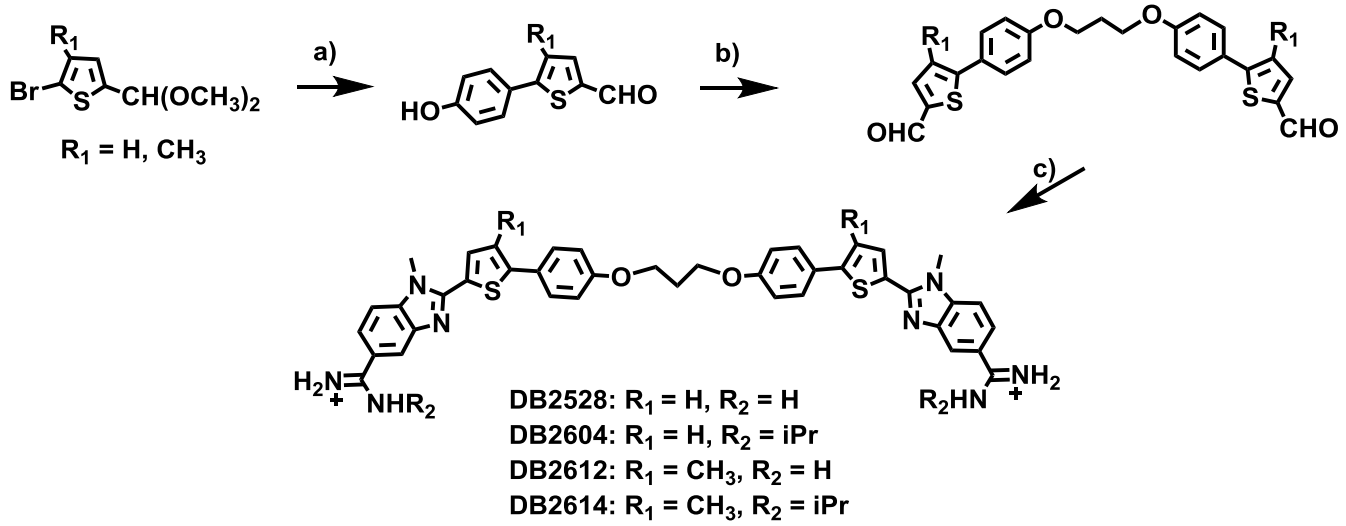

Scheme S1. Synthesis of two G·C bps binders. Reagents and conditions: a) i. 4-hydroxyphenyl-boronic acid, $Pd(PPh_3)_4$, 2 M aqueous K_2CO_3, EtOH, reflux ii. HCl, H_2O. b) dibromoalkane, K_2CO_3, DMF, 80 °C. c) 3-amino-4-(methylamino)benzamidine or 3-amino-4-(methylamino)-*N*-isopropylbenzamidine, 1,4-benzoquinone, DMF, EtOH, reflux.

All commercial reagents were used without purification. Melting points were determined on a Mel-Temp 3.0 melting point apparatus, and are uncorrected. TLC analysis was carried out on silica gel 60 F254 precoated aluminum sheets using UV light for detection. ^{1}H and ^{13}C NMR spectra were recorded on a Bruker 400 MHz spectrometer using the indicated solvents. Mass spectra were obtained from the Georgia State University Mass Spectrometry Laboratory, Atlanta, GA. The compounds reported as salts contain waters of hydration and in each case a water signal was noted in the ^{1}H-NMR spectra. Elemental analyses were performed by Atlantic Microlab Inc., Norcross, GA.

General procedure for the amidinobenzimidazole synthesis:

A mixture of dialdehyde (0.0004 mol) and 4-amidino-1, 2-diaminobenzene hydrochloride or 4-*N*-isopropylamidino-1-methylamino)-2-aminobenzene hydrochloride or 4-*N*-isopropylamidino-1, 2-diaminobenzene hydrochloride (0.0008 mol) in 5 mL anhydrous DMF under nitrogen was stirred at rt for

15 min., followed by addition of 35 mL anhydrous ethanol and heated at reflux for 15 min., 1,4-benzoquinone (0.108 g, 0.001 mol) was then added and the mixture was heated under reflux for 12-18 hr. The reaction mixture was concentrated under reduced pressure to 5 mL and stirred with 75 ml acetone for 2 h, filtered, washed with acetone, ether and dried under reduced pressure. The dark solid obtained was suspended in anhydrous ethanol or methanol, heated until dissolved, filtered, concentrated under reduced pressure to 15 mL, diluted with ether, filtered, washed with ether and the solid was dried under reduced pressure at 75 °C for 12 h, to provide dark colored dihydrochloride in 68-75% yield. In the case of DB2528 a tetrahydrochloride was prepared by treating an ethanol solution of the dihydrochloride with saturated EtOH-HCl.

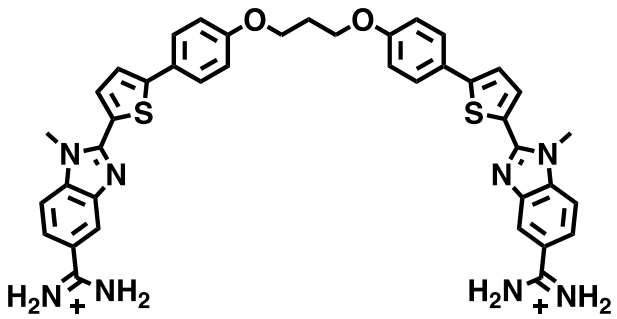

2,2'-(((Propane-1,3-diylbis(oxy)) bis(4,1-phenylene)) bis(thiophene-5,2-diyl)) bis(1-methyl-1H-benzo[d]imidazole-5-carboximidamide) tetrahydrochloride (DB 2528).

To a stirred solution of 5-bromothiophene-2-carboxaldehyde dimethyl acetal (7.11 g, 0.03 mol) and 4-hydroxyphenylboronic acid (4.52 g, 0.033 mol) in 70 mL 1,4-dioxane, under N_2, was added 30 ml 2M aqueous K_2CO_3 and 30 ml ethanol, followed by $Pd(PPh_3)_4$ (0.69 g, 2 mol %), and the mixture was heated at reflux for 12 h (TLC monitored). The solvent was removed, the residue was stirred in ice-water and acidified with HCl and external cooling. The yellow solid which separated, was washed with water, dried and recrystallized from DCM-methanol to yield 5-(4-hydroxyphenyl)-thiophene-2-carboxaldehyde as a yellow solid 4.16 g (68%), mp 210-12 °C dec.; ^{1}H NMR (DMSO-d_6): 10.03 (s, 1H), 9.85 (s, 1H), 7.98 (d, 1H, J = 3.6 Hz), 7.64 (d, 2H, J = 8.0 Hz), 7.55 (d, 1H, J = 3.6 Hz), 6.86 (d, 2H, J = 8.0 Hz); ^{13}C NMR (DMSO-d_6): 184.1, 159.5, 154.2, 141.0, 140.0, 128.3, 124.0, 123.8, 116.6; HRMS-ESI calcd for $C_{11}H_8O_2NaS$: 227.0139 [M^+]. Found m/z 227.0133.

5-(4-Hydroxyphenyl)-thiophene-2-aldehyde (2.04 g, 0.01 mol), 1,3-dibromopropane (1.01 g, 0.005 mol), and anhydrous K_2CO_3 (2.07 g, 0.015 mol) in 5-6 mL DMF was heated at 70 °C for 8 h [(TLC monitored). The mixture was diluted with ice water (30 mL), the precipitated solid was filtered, washed with water, and dried. The solid was suspended in DCM-methanol (50:10) mixture, stirred, filtered, washed with ether and dried under reduced pressure to yield the dialdehyde as a greenish yellow solid 1.09 g (48%), mp 218-20 °C dec.; ^{1}H NMR (DMSO-d_6/75 °C): 9.89 (s, 2H), 7.95 (d, 2H, J = 4.0 Hz), 7.71 (d, 4H, J =

8.0 Hz), 7.55 (d, 2H, J = 4.0 Hz), 7.07 (d, 4H, J = 8.0 Hz), 4.25 (t, 4H, J = 6.4 Hz), 2.24 (quintet, 2H, J = 6.4 Hz); ^{13}C NMR (DMSO-d_6/78°C): 182.8, 159.3, 152.5, 140.8, 138.1, 127.2, 125.0, 123.4, 115.1, 64.4, 28.2; HRMS-ESI: calcd for $C_{25}H_{21}O_4S_2$: 449.0876 [M^++1]. Found *m/z* 449.0854

Following the general procedure the dialdehyde 0.179 g (0.0004 mol) provided the diamidine as dark grey solid 0.247 g (69%), mp >320 °C dec.; ^{1}H NMR (DMSO-d_6): 9.24 (br, 4H), 9.07 (br, 4H), 8.24 (s, 2H), 7.84-7.78 (m, 6H), 7.71 (d, 4H, J = 8.0 Hz), 7.54 (brs, 2H), 7.09 (d, 4H, J = 8.0 Hz), 4.23 (t, 4H, J = 5.6 Hz), 4.11 (brs, 6H), 2.25 (quintet, 2H, J = 5.6 Hz); ^{13}C NMR (DMSO-d_6): 165.8, 158.6, 149.4, 146.7, 141.5, 139.9, 129.7, 129.1, 126.7, 125.4, 123.1, 121.5, 120.9, 118.7, 115.1, 110.3, 64.4, 31.6, 28.3; HRMS-ESI: calcd for $C_{41}H_{38}N_8O_2S_2$ 369.1274 [M^++1]/2. Found *m/z* 369.1232; Anal. calcd for $C_{41}H_{36}N_8O_2S_2$-4HCl-H_2O; C, 54.66; H, 4.69; N, 12.44. Found: C, 54.79; H, 4.54; N, 12.72.

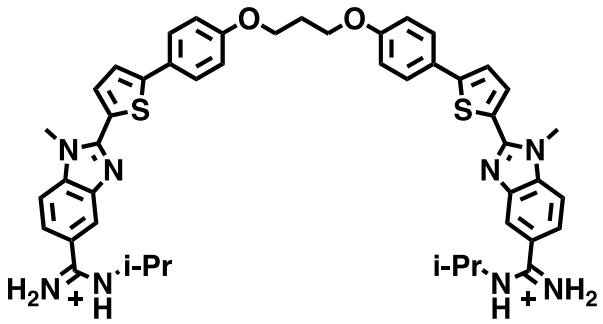

2,2'-(((Propane-1,3-diylbis(oxy))bis(4,1-phenylene))bis(thiophene-5,2-diyl))bis(N-isopropyl-1-methyl-1H-benzo[d]imidazole-5-carboximidamide) dihydrochloride (**DB 2604).**

Following the general procedure the dialdehyde 0.179 g (0.0004 mol) yielded the diamidine as reddish brown solid, 0.28 9 g (74%); mp >330 °C dec.; ^{1}H NMR (DMSO-d_6): 9.56 (s, 1H), 9.54 (s, 1H), 9.44 (br, 2H), 9.07 (br, 2H), 8.09 (s, 2H), 7.89-7.86 (m, 4H), 7.73 (d, 4H, J = 8.8 Hz), 7.65 (d, 2H, J = 8.8 Hz), 7.60 (d, 2H, J= 4.0 Hz), 7.09 (d, 4H, J= 8.8 Hz), 4.22 (t, 4H, J = 6.4 Hz), 3.95-4.0 (m, 8H), 2.24 (quintet, 2H, J = 6.4 Hz), 1.32 (d, 12H, J= 6.4 Hz); ^{13}C NMR (DMSO-d_6): 162.0, 158.7, 149.3, 146.7, 141.3, 139.6, 129.8, 129.3, 126.8, 125.4, 123.3, 122.6, 121.9, 118.9, 115.1, 110.2, 64.4, 44.8, 31.7, 28.4, 20.9; HRMS-ESI: calcd for $C_{47}H_{50}N_8O_2S_2$: 411.1744 [M^++2]/2. Found *m/z* 411.1732; Anal. calcd for $C_{47}H_{48}N_8O_2S_2$-2HCl-4.75H_2O: C, 57.33; H, 5.93; N, 11.53. Found: C, 57.62; H, 6.12; N, 11.4.

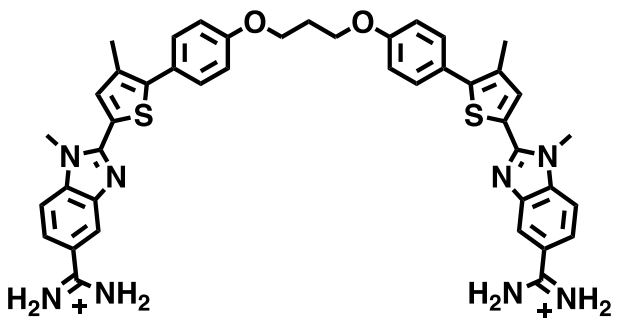

2,2'-(((Propane-1,3-diylbis(oxy))bis(4,1-phenylene))bis(4-methylthiophene-5,2-diyl))bis(1-methyl-1H-benzo[d]imidazole-5-carboximidamide) dihydrochloride (DB 2612).

5-(4-Hydroxyphenyl)-4-methyl thiophene-2-aldehyde was prepared following the procedure for the aldhyde precursor for DB2528 providing 4.25 g (65%) of a yellow solid; mp 170-2 °C; ^{1}H NMR (DMSO-d_6): 9.93 (br, 1H), 9.82 (s, 1H), 7.86 (s, 1H), 7.41 (d, 2H, J = 8.0 Hz), 6.89 (d, 2H, J = 8.0 Hz), 3.21 (s, 3H); ^{13}C NMR (DMSO-d_6): 184.1, 158.7, 148.4, 142.3, 139.6, 134.3, 130.5, 124.0, 116.3, 15.4; HRMS-ESI calcd for $C_{12}H_{10}O_2NaS$: 241.0376 [M^+]. Found m/z 241.0299.

5-(4-Hydroxyphenyl)-4-methyl thiophene-2-aldehyde (2.18 g, 0.01mol), 1,3-dibromopropane (1.01 g, 0.005 mol), and anhydrous K_2CO_3 (2.07 g, 0.01 mol) in 35 mL ethanol was allowed to reflux and worked up as described for the dialdehyde precursor of DB 2528; the dialdehyde, 1.07 g (45%**),** was obtained after chromatography over silica get with DCM elution as red crystals; mp 30-31 °C, ^{1}H NMR (DMSO-d_6): 9.84 (s, 2H), 7.88 (s, 2H), 7.51 (d, 4H, J = 8.0 Hz), 7.09 (d, 4H, J = 8.0 Hz), 4.25 (br, 4H), 2.32 (s, 6H), 2.25 (br, 2H); ^{13}C NMR (DMSO-d_6): 183.7, 158.9, 147.2, 141.6, 139.5, 134.2, 130.0, 125.1, 115.0, 64.3, 28.5, 14.8; HRMS-ESI: calcd for $C_{27}H_{25}O_4S_2$: 477.1189 [M^++1]. Found *m/z* 477.1196.

Following the general procedure the dialdehyde 0.19 g (0.0004 mol) yielded the diamidine as a brownish grey solid, 0.25 g (71%); mp >320 °C dec.; ^{1}H NMR (DMSO-d_6): 9.37 (brs, 4H), 9.11 (brs, 4H), 8.20 (s, 2H), 7.89 (d, 2H, J = 8.4 Hz), 7.79 (s, 2H), 7.76 (d, 2H, J = 8.4Hz), 7.52 (d, 4H, J = 8.4 Hz), 7.12 (d, 4H, J = 8.4 Hz), 4.24 (t, 4H, J = 5.6 Hz), 4.12 (s, 6H), 2.37 (s, 6H), 2.25 (quintet, 2H, J = 5.6Hz); ^{13}C NMR (DMSO-d_6): 165.9, 158.3, 149.6, 141.7, 140.8, 140.1, 133.4, 132.7, 129.6, 128.0, 125.4, 121.6, 121.1, 118.9, 114.9, 110.6, 64.4, 31.8, 28.5, 14.5; HRMS-ESI: calcd for $C_{43}H_{42}N_8O_2S_2$: 383.1431 [M^++1]/2. Found *m/z* 383.1418; Anal. calcd for $C_{43}H_{40}N_8O_2S_2$-2HCl-2.5H_2O: C, 58.26; H 5.19; N, 12.30. Found: C, 58.49; H, 5.36; N, 12.69.

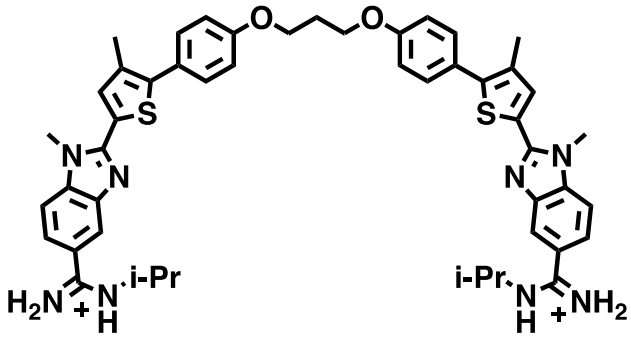

2,2'-(((Propane-1,3-diylbis(oxy))bis(4,1-phenylene))bis(4-methylthiophene-5,2-diyl))bis(N-isopropyl-1-methyl-1H-benzo[d]imidazole-5-carboximidamide) dihydrochloride (DB 2614).

Following the general procedure the dialdehyde 0.19 g (0.0004 mol) provided the diamidine as purple brown solid, 0.278 g (72%); mp >320 °C dec.; ^{1}H NMR (DMSO-d_6): 9.53 (s, 1H), 9.51 (s, 1H), 9.41 (brs,

2H), 9.03 (brs, 2H), 8.07 (d, 2H, J = 1.6 Hz), 7.87 (d, 2H, J = 8.8Hz), 7.79 (s, 2H),7.64 (dd, 2H, J = 1.6 Hz, J = 8.8 Hz), 7.52 (d, 4H, J = 8.8 Hz), 7.12 (d, 4H, J = 8.8 Hz), 4.25 (t, 4H, J = 6.0 Hz), 4.13 (s, 6H), 4.09-4.07 (septet, 2H, J = 6.4 Hz), 2.37 (s, 6H), 2.56 (quintet, 2H, J = 6.0Hz), 1.31 (d, 12H, J = 6.4 Hz); ^{13}C NMR (DMSO-d_6): 162.0, 158.2, 149.3, 141.5, 140.7, 139.6, 133.3, 132.6, 129.5, 128.0, 125.4, 122.6, 121.9, 118.9, 114.8, 110.3, 64.4, 44.8, 31.8, 28.4, 20.9, 14.5; HRMS-ESI: calcd for $C_{49}H_{54}N_8O_2S_2$: 425.1990 [M^++2]/2. Found *m/z* 425.1890; Anal. calcd for $C_{49}H_{52}N_8O_2S_2$-2HCl-2.5H_2O: C, 60.92; H 5.93; N, 11.30. Found: C, 60.85; H, 6.14; N, 11.58.

Biophysical Experimental

Materials

In the DNA thermal melting (T_m), circular dichroism (CD), fluorescence anisotropy, and electrospray ionization mass spectrometry (ESI-MS) experiments, the hairpin oligomer sequences were used as shown in Table S1. In SPR experiments, 5′-biotin labeled hairpin DNA oligomers were used. All DNA oligomers were obtained from Integrated DNA Technologies, Inc. (IDT, Coralville, IA) with reverse-phase HPLC purification and mass spectrometry characterization.

The buffer used in T_m, CD, and fluorescence experiments was 50 mM Tris-HCl, 100 mM NaCl, 1 mM EDTA, pH 7.4 (TNE 100). The biosensor-surface plasmon resonance (SPR) experiments were performed in filtered, degassed TNE 100 with 0.05% (v/v) surfactant P20. 50 mM ammonium acetate buffer with 10% MeOH was used in ESI-MS experiments.

UV-vis Thermal Melting (T_m)

DNA thermal melting experiments were performed on a Cary 300 Bio UV-vis spectrophotometer (Varian). The concentration of each hairpin DNA sequence was 3 μM in TNE 100 using 1 cm quartz cuvettes. The solutions of DNA and ligands were tested with the ratio of 2:1 [ligand] : [DNA]. All samples were increased to 95 °C and cooled down to 25 °C slowly before each experiment. The spectrophotometer was set at 260 nm with a 0.5 °C/min increase beginning at 25 °C, which is below the DNA melting temperature and ending above it at 95 °C. The absorbance of the buffer was subtracted, and a graph of normalized

absorbance versus temperature was created using KaleidaGraph 4.0 software. The ΔT_m values were calculated using a combination of the derivative function and estimation from the normalized graphs.

Biosensor-Surface Plasmon Resonance (SPR)

SPR measurements were performed with a four-channel Biacore T200 optical biosensor system (GE Healthcare, Inc., Piscataway, NJ). A streptavidin-derivatized (SA) CM5 sensor chip was prepared for use by conditioning with a series of 180 s injections of 1 M NaCl in 50 mM NaOH (activation buffer) followed by extensive washing with HBS buffer (10 mM HEPES, 150 mM NaCl, 3 mM EDTA, and 0.05% P20, pH 7.4). Biotinylated-DNA samples (AAAATTTT, AAAAGTTTT, GAAG, GAAAC, GAAAAC, and GAAAAAC hairpins, Table S1) of 25-30 nM were prepared in HBS buffer and immobilized on the flow cell surface by noncovalent capture as previously described.[1] Flow cell 1 was left blank as a reference, while flow cells 2−4 were immobilized separately by manual injection of biotinylated-DNA stock solutions (flow rate of 1 µL/min) until the desired amount of DNA response units (RU) was obtained (250−300 RU). Ligand solutions were prepared with degassed and filtered TNE 100 with 0.05% (v/v) surfactant P20 by serial dilutions from a concentrated stock solution. Typically, a series of different ligand concentrations (2 nM to 500 nM) were injected over the DNA sensor chip at a flow rate of 100 µL/min for 180 s, followed by buffer flow for ligand dissociation (600−1800 s). After each cycle, the sensor chip surface was regenerated with a 10 mM glycine solution (pH 2.5) for 30 s followed by multiple buffer injections to yield a stable baseline for the following cycles. RU_{obs} was plotted as a function of free ligand concentration (C_{free}), and the equilibrium binding constants (K_A) were determined either with a one-site binding model, where $r = (RU_{obs}/RU_{max})$ represents the moles of bound compound/mol of DNA hairpin duplex and K is macroscopic binding constant.

$$\boldsymbol{r = K * C_{free}/1 + K * C_{free}} \qquad \textbf{(1)}$$

RU_{max} can be used as a fitting parameter, and the obtained value compared to the predicted maximal response per bound ligand can also be used to independently evaluate the stoichiometry.[2] Kinetic analyses were performed by globally fitting the binding results for the entire concentration series using a standard 1:1 kinetic model with integrated mass transport-limited binding parameters as described previously.[3]

Fluorescence Emission Spectroscopy and Anisotropy

Fluorescence spectra were recorded on a Cary Eclipse Spectrophotometer, with excitation and emission slit width typically fixed at 10, 10 nm. The free compound solutions at different concentrations were prepared in TNE 100, and DNA sequence aliquots were added from a concentrated stock. Titration

spectra were collected after allowing an incubation time of 10 min. The excitation wavelength is based on molecular absorbance from UV-vis spectroscopy. Emission spectra were monitored at the fluorescence excitation wavelength at 25 °C.

Fluorescence anisotropy (r) measures the extent of polarization of the fluorescence emission of a system in solution when excited with polarized light. It is directly related to the rotational diffusion of the system and is low for small and flexible molecules (higher depolarization), and increases when larger complexes are formed (slower rotational movement, smaller depolarization).[4] Therefore, the change in fluorescence anisotropy can be used to monitor a binding reaction.[5] This is particularly convenient for systems where no or small changes in fluorescence intensity is observed between the free and bound states. The fluorescence anisotropy is defined in the equation:

$$\boldsymbol{r = \frac{Ivv - GIvh}{Ivv + 2GIvh}}\ \boldsymbol{, G = \frac{Ihv}{Ihh}} \qquad \textbf{(2)}$$

where I_{vv} is the fluorescence emission intensity measured for vertically polarized excitation and vertically polarized emission. I_{vh} is the intensity measured for vertically polarized excitation and horizontally polarized emission, and G is a correction factor.

Depending on the parameters achieved from the previous step, add an appropriate concentration of ligands until the total intensity of emission wavelength is ~ 400. Record that concentration. Place blank cuvette containing TNE 100 in the instrument. Collect the spectrum using parameters obtained from the previous part, double check the emission spectra. The polarizer (Agilent Technologies, Manual Polarizer Accessory) was installed to the system and set the excitation and emission wavelength of compound same as the previous scan spectrum. The slit width fixed same as [10, 10 nm] and the average time of reading was set as 50 s. Read I_{vv}, I_{vh} of the buffer as a blank sample. The I_{hh}, I_{hv} of ligand only solution with the concentration same as the record was read to calculate the G of ligand. The I_{vv} and I_{vh} of each titration sample including ligand only were read to be made into scatter plot and fit the data to get the K_D value in KaleidaGraph 4.0 software.

Circular Dichroism (CD)

Circular dichroism experiments were performed on a Jasco J-810 CD spectrometer in 1 cm quartz cuvette at 25 °C. A buffer scan as a baseline was collected first in the same cuvette and subtracted from the scan of following samples. The hairpin DNA sequence GAAAC or AAAATTTT (5 μM),Table S1, in TNE 100 was added to the cuvette prior to the titration experiments and then the compound was added to the DNA solution and incubated for 10 min to achieve equilibrium binding for the DNA-ligand complex

formation. For each titration point, four spectra were averaged from 500 to 220 nm wavelength with scan speed 50 nm/min, with a response time of 1 s. Baseline-subtracted graphs were created using the KaleidaGraph 4.0 software.

Competition Electrospray Ionization Mass Spectrometry (ESI-MS)

Electrospray Ionization Mass Spectrometry (ESI-MS) analyses were performed on a Waters Q-TOF micro Mass Spectrometer (Waters Corporate, Milford, MA) equipped with an electrospray ionization source (ESI) in a negative ion mode. DNA sequences AAAATTTT, AAAAGTTTT, GAAC, GAAAC, GAAAAC and GAAAAAC, Table S1, for ESI-MS experiments were purified by dialyzing it in 50 mM ammonium acetate buffer (pH 6.7) at 4 ºC with 3x buffer exchange. Test samples were prepared in 50 mM ammonium acetate with 10% v/v methanol at pH 6.7 and introduced into the ion source through direct infusion at 5 µl/min flow rate. The competitive experiments were done by mixing a ligand and DNAs with different sequences at different ratios. The instrument parameters were typically as follows: capillary voltage of 2800 V, sample cone voltage of 30 V, extraction cone voltage of 1.0 V, desolvation temperature of 70 °C, and source temperature of 100 °C. Nitrogen was used as nebulizing and drying gas. A multiply charged spectra were acquired through a full scan analysis at mass range from 300-2500 Da and then deconvoluted to the spectra presented. MassLynx 4.1 software was used for data acquisition and deconvolution.

Ab-Initio Calculations and Molecular Dynamic (MD) Simulation

Optimization and electrostatic potential calculations were performed for the DB2528 molecule using DFT/B3LYP theory with the 6-31+G* basis set in Gaussian 09 (Gaussian, Inc., 2009, Wallingford, CT) with Gauss-view 5.09.[6] Partial charges were derived using the RESP fitting method (Restrained Electrostatic potential). [7,8]

AMBER 14 (Assisted Model Building with Energy Refinement) software suite was used to perform molecular dynamic (MD) simulations.[9] Canonical *B*-form *ds*[(5'-CCAAAGAAACTTTGG-3')(5'-CCAAAGTTTCTTTGG-3')] DNA was built in Nucleic Acid Builder (NAB) tool in AMBER. AMBER preparation and force field parameter files required to run molecular dynamic simulations for DB2528 molecule were produced using ANTECHAMBER.[10] Specific atom types assigned for DB2528 molecule were adapted from the ff99 force field. Most of the force field parameters for DB2528 molecule were derived from the existing set of bonds, angles and dihedrals for the similar atom types in parm99 and GAFF force fields. Some dihedral angle parameters were obtained from previously reported parametrized data. [11,12] Parameters of DB2528 in frcmod file are listed at the Figure S6.

AutoDock Vina program was used to dock the DB2528 in the minor groove of DNA to obtain the initial structure for DB2528-DNA complex.[13] MD simulations were performed in explicit solvation

conditions where the DNA-DB2528 complex was placed in a truncated octahedron box filled with TIP3P water using xleap program in AMBER. Sodium ions were used to neutralize the system. A 10 Å cutoff was applied on all van der Waals interactions. The MD simulation was carried out using the Sander module with SHAKE algorithm applied to constrain all bonds. Initially, the system was relaxed with 500 steps of steepest-descent energy minimization. The temperature of the system was then increased from 0 K to 310 K for over 10 ps under constant-volume conditions. In the final step, the production run on the system was subsequently performed for 300 ns under NPT (constant-pressure) conditions. Coordinate file of DB2528-DNA complex along with water molecules in proximity is also attached (terminal bp is not included due to fraying at the ends of DNA).

Tables and Figures

Table S1. All sequences used in this paper. [a]

Name	Sequences
AAAATTTT	5'-CCAAAATTTTGCTCTCAAAATTTTGG-3'
AAAAGTTTT	5'-CCAAAAGTTTTGCTCTCAAAACTTTTGG-3'
GC	5'-CCAAAAGCTTTTGCTCTCAAAAGCTTTTGG-3'
GAC	5'-CCAAAGACTTTGCTCTCAAAGTCTTTGG-3'
GAAC	5'-CCAAAGAACTTTGCTCTCAAAGTTCTTTGG-3'
GAAG	5'-CCAAAGAAGTTTGCTCTCAAACTTCTTTGG-3'
GAAAC	5'-CCAAAGAAACTTTGCTCTCAAAGTTTCTTTGG-3'
GAAAG	5'-CCAAAGAAAGTTTGCTCTCAAACTTTCTTTGG-3'
GATAC	5'-CCAAGATACTTGCTCTCAAGTATCTTGG-3'
CAAAG-1	5'-CCAAACAAAGTTTGCTCTCAAACTTTGTTTGG-3'
CAAAG-2	5'-CCAACAAAGTTGCTCTCAACTTTGTTGG-3'
GAAAAC	5'-CCAAAGAAAACTTTGCTCTCAAAGTTTTCTTTGG-3'
GAATTC	5'-CCAAGAATTCTTGCTCTCAAGAATTCTTGG-3'
GAAAAAC-1	5'-CCAAGAAAAACTTGCTCTCAAGTTTTTCTTGG-3'
GAAAAAC-2	5'-CCAAAGAAAAACTTTGCTCTCAAAGTTTTTCTTTGG-3'

a: The loop circle is shown underlined. The 5'-biotin labeled sequences were used in SPR experiments.

Table S2. Thermal melting studies ΔT_m (℃) of studied compounds with pure AT and mixed DNA sequences. [a]

ΔT_m (℃) DNA T_m (℃)[b]	AAAA TTTT 64	AAAA G TTTT 67	AAAA GC TTTT 69	AAA GAC TTT 70	AAA GAAC TTT 71	AAA GAAAC TTT 69	AAA GAAAAC TTT 70	AA GAAAAAC TT 70
DB2528	**1**	**2**	**1**	**2**	**1**	**9**	**6**	**6**
DB2604	**2**	**3**	**1**	**2**	**2**	**9**	**6**	**6**
DB2612	**1**	**<1**	**1**	**1**	**1**	**2**	**1**	**1**
DB2614	**2**	**2**	**1**	**1**	**2**	**6**	**5**	**5**

a: ΔT_m=T_m (the complex)-T_m (the native DNA). 3 μM DNA sequences were tested in TNE 100 with the ratio of 2:1 [ligand] : [DNA]. An average of two independent experiments with a reproducibility of ±0.5 ℃. Full DNA sequences can be seen in Table S1.

b: The values are the melting temperature of DNAs only used to calculate the relative data.

Table S3. Summary of binding affinity (K_D, nM) for the interaction of all test compounds with biotin-labeled DNA sequences using biosensor-SPR method [a]

K_D (nM)	AAAA TTTT	AAAA G TTTT	AAA GAAAC TTT	AAA GAAAAC TTT	AA GAAAAAC TT	AAA GAAG TTT
DB2528	**NB**	**NB**	**5**	**6**	**--**	**149**
DB2604	**150**	**--**	**12**	**--**	**30**	**--**
DB2612	**--**	**--**	**50**	**--**	**100**	**--**
DB2614	**--**	**--**	**85**	**--**	**98**	**--**

a: All the results in this table were investigated in TNE 100 with 0.05% P20 at a 100 μL min^{-1} flow rate. "--" experiment not done, "NB" no binding. The listed binding affinities are an average of two independent experiments carried out with two different sensor chips and the values are reproducible within 10% experimental errors.

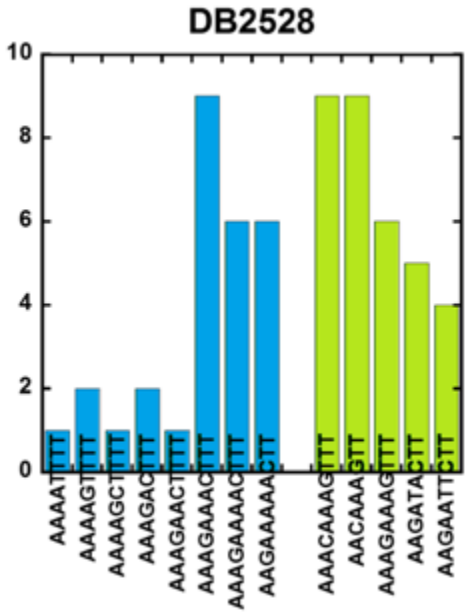

Figure S1. Comparisons of thermal melting results (ΔT_m, °C) of DB2528 with pure AT and mixed DNA sequences. ΔT_m = T_m (the complex) - T_m (the native DNA). 3 μM DNA sequences were studied in TNE 100 with the ratio of 2:1 [ligand]:[DNA]. An average of two independent experiments with a reproducibility of ±0.5 °C.

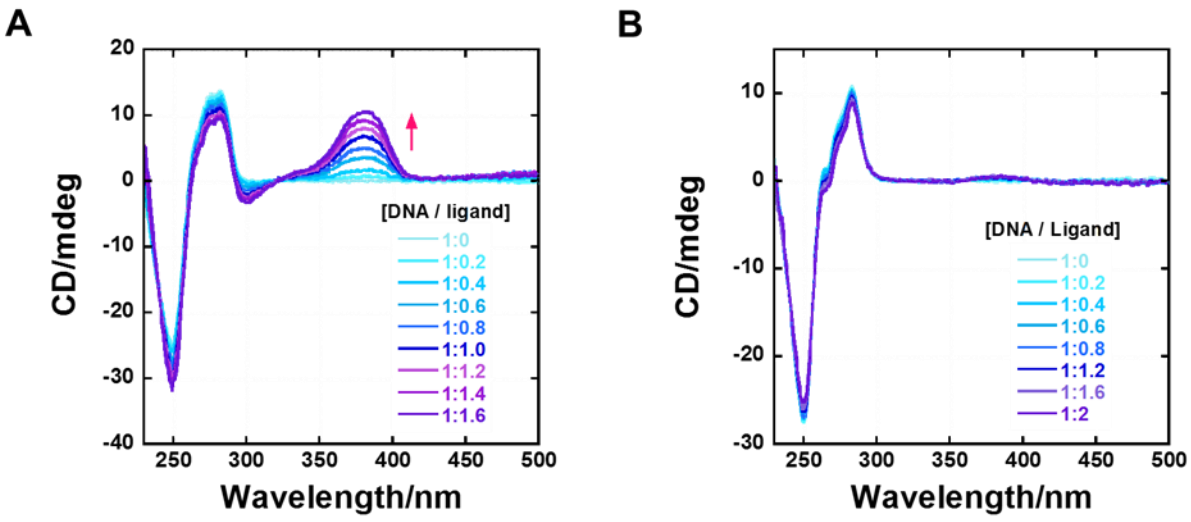

Figure S2. Circular dichroism titration spectra of DB2528. DB2528 was titrated into 5 μM sequence A) AAAGAAACTTT; B) AAAATTTT (Table S1). Arrow indicates the ligand induced spectral changes in DNA during titration.

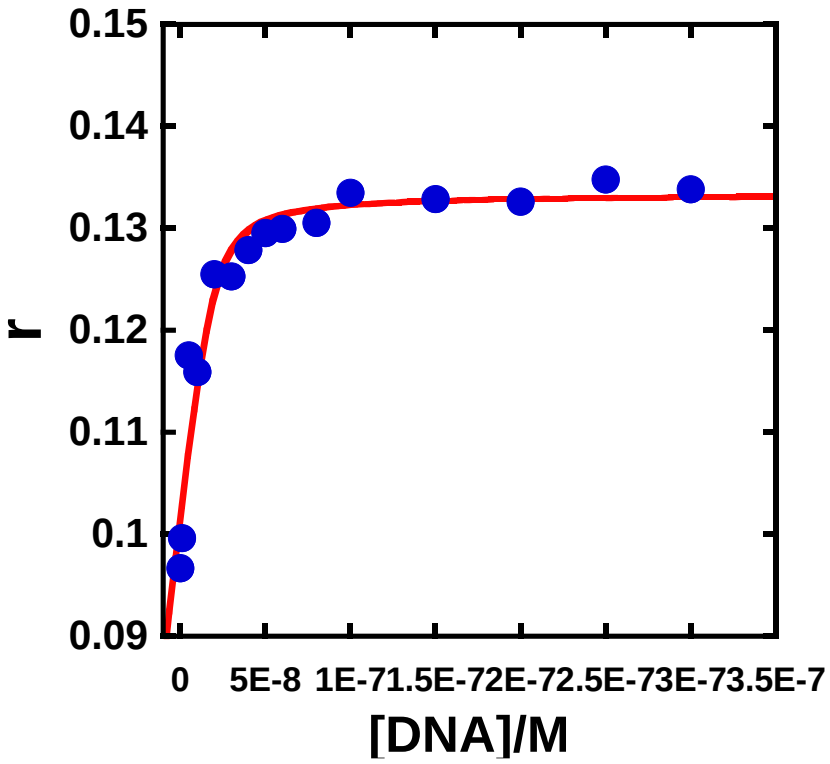

Figure S3. Fluorescence Anisotropy (FA) binding curve between 20 nM DB2604 and sequence GAAAC in TNE 100. Ex_{max} = 365 nm; Em_{max} = 468 nm; slit width: [10, 10 nm]. The FA collection concentration points are 0, 1, 5, 10, 20, 30, 40, 50 ,60, 80, 100, 150, 200, 250, 300 nM.

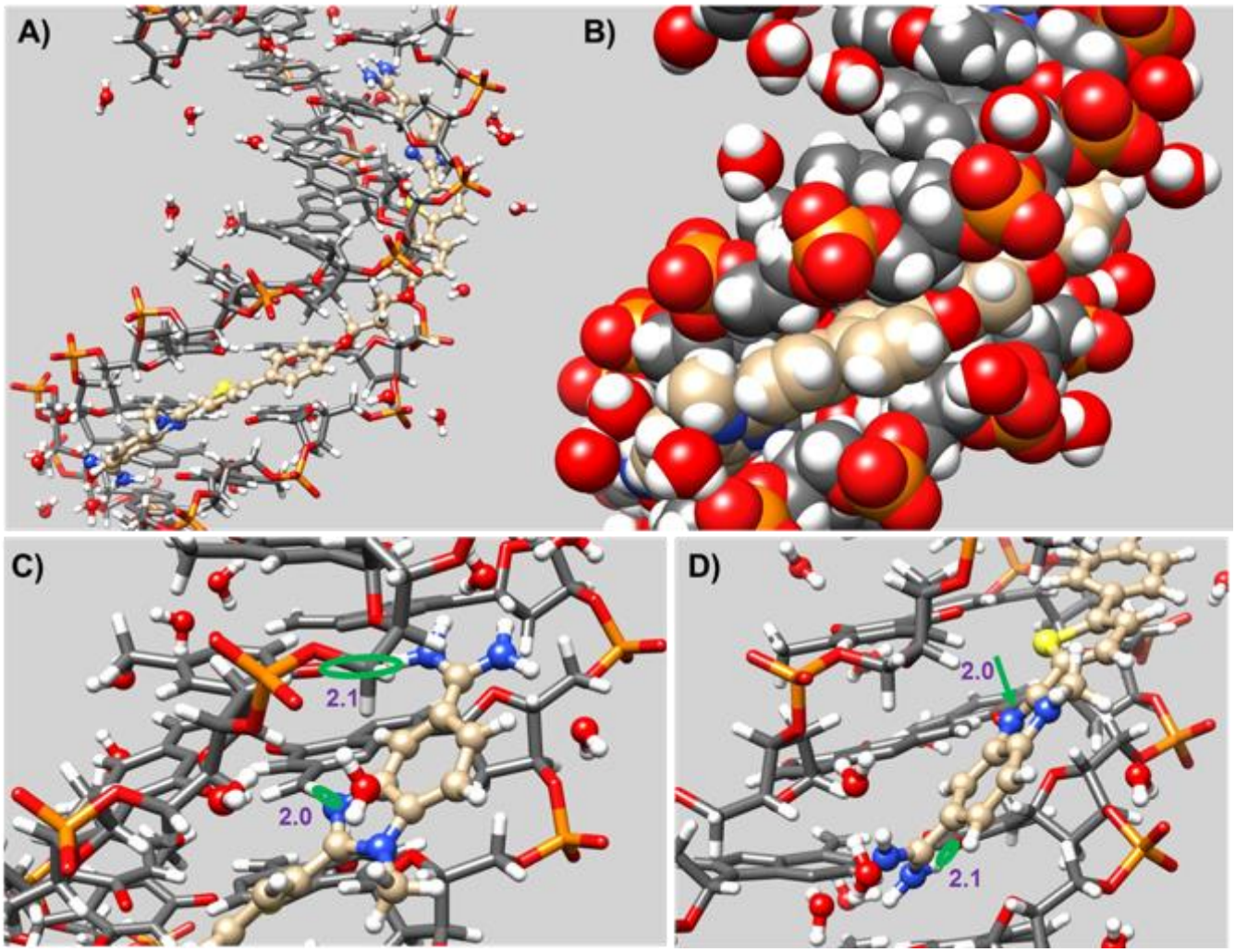

Figure S4: A) Full view of the DB2528-DNA complex along with the water molecules in vicinity of complex. B) Space fill representation of DB2528-DNA complex. C) Upper part of the complex with H-bond of G6-NH and T26-O2 of DNA with N of *N*-MeBI and NH of amidine of DB2528 respectively is market in green (in Å). D) Lower part of the complex with H-bond interaction of G21-NH and T11-O2 of DNA with N of *N*-MeBI and NH of amidine respectively, is marked in the green (in Å).

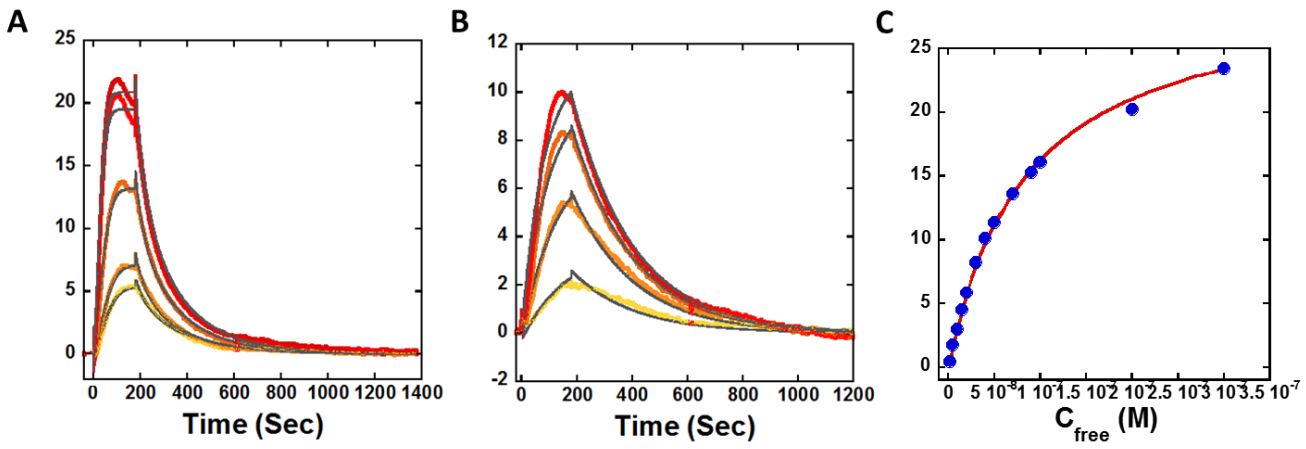

Figure S5: Representative SPR sensorgrams for A) DB2604 and B) DB2612 in the presence of GAAAC hairpin DNA, concentrations of DB2604 from bottom to top are 20, 40, 70, and 90 nm, and for DB2612 from bottom to top are 15, 40, 70 and 90 nm. C) Steady-state binding plots for DB2614 with sequence GAAAC. The data are fitted to a steady state binding function using a 1:1 model to determine equilibrium binding constants. In (A) and (B) the solid black lines are best-fit values for global kinetic fitting of the results with a single site function.

Figure S6. Frcmod file of the DB2528 molecule.

```
remark goes here
MASS
N2 14.01        0.530           parm99
H  1.008        0.161           parm99
CA 12.01        0.360           parm99
HA 1.008        0.167           parm99
CB 12.01        0.360           parm99
N* 14.01        0.530           parm99
NB 14.01        0.530           parm99
CK 12.01        0.360           parm99
H1 1.008        0.135           parm99
CT 12.01        0.878           parm99
C* 12.01        0.360           Sp2 carbons in non-pure aromatic systems GAFF
S  32.06        2.900           Sp3 S in thio-ester and thio-ether GAFF
OS 16.00        0.465           parm99

BOND
CA-CA  469.0    1.400       parm99
CA-CB  469.0    1.404       parm99
CA-HA  367.0    1.080       parm99
CA-N2  481.0    1.340       parm99
CB-CB  520.0    1.370       parm99
CB-N*  436.0    1.374       parm99
CB-NB  414.0    1.391       parm99
CK-N*  440.0    1.371       parm99
CK-NB  529.0    1.304       parm99
CK-C*  418.3    1.4290      SOURCE1     740     0.0069 cc-cc gaff similar to gaussian bond
H -N2  434.0    1.010       parm99
CT-H1  340.0    1.090       parm99
CA-C*  411.7    1.4340      SOURCE1      80     0.0000 ca-cc gaff
C*-C*  418.3    1.4290      SOURCE1     740     0.0069 cc-cc gaff
C*-S   279.3    1.7370      SOURCE3      52 0.0194 cc-ss gaff
C*-HA  347.2    1.0850      SOURCE3     740     0.0039 cc-ha gaff
CA-OS  372.4    1.3730      gaff, ca-os
CT-OS  320.0    1.410       parm99
CT-CT  310.0    1.526       JCC,7,(1986),230; AA, SUGARS parm99

ANGLE
N2-CA-N2    70.0      120.00    parm99
H -N2-H     35.0      120.00    parm99
CA-CA-N2    70.0      119.99    parm99, CM-CA-N2, Gaussian-angle
CA-N2-H     50.0      120.00    parm99
CA-CA-CA    63.0      120.00    parm99
CA-CA-HA    50.0      120.00    parm99
H1-CT-H1    35.0      109.50    parm99
CA-CB-CB    63.0      117.30    parm99
CA-CB-NB    70.0      132.40    parm99
CB-CB-NB    70.0      110.40    parm99
CB-CB-N*    70.0      106.20    parm99
CB-N*-CK    70.0      105.40    parm99
```

CB-NB-CK 70.0 103.80 parm99
N*-CK-NB 70.0 113.90 parm99
CA-C*-C* 67.66 111.04 SOURCE3 9 7.9455 ca-cc-cc GAFF
C*-C*-CK 66.24 121.77 CORR c2-cc-cc GAFF
C*-C*-C* 67.88 110.70 SOURCE3 54 3.4091 cc-cc-cc GAFF
CK-N*-CT 70.0 128.80
CB-N*-CT 70.0 125.80
H1-CT-N* 50.0 109.50 changed based on NMA nmodes
C*-S -C* 67.01 89.91 SOURCE3 11 2.2164 cc-ss-cc
CA-C*-S 62.30 120.51 CORR 43 ca-cc-ss GAFF
C*-C*-HA 47.14 120.86 CORR 1751 cc-cc-ha GAFF
S -C*-CK 62.45 120.12 CORR 31 cc-cc-ss
S -C*-C* 62.45 120.12 CORR 31 cc-cc-ss
C*-CK-N* 67.53 121.69 CORR 105 cc-cc-nc GAFF
C*-CK-NB 67.53 121.69 CORR 105 cc-cc-nc GAFF
CA-CB-N* 70.0 132.40 CA-CB-NB parm99
CA-CA-CB 63.0 120.00 changed from 85.0 bsd on C6H6 nmodes
CB-CA-HA 50.0 120.00
CA-CA-C* 65.99 120.10 SOURCE3 103 0.3451 ca-ca-cc
CT-OS-CA 62.3 119.76 gaff, c3-os-ca, Gaussian-angle
H1-CT-OS 50.0 109.50 parm99
H1-CT-H1 35.0 109.50 parm99
CT-CT-H1 50.0 109.50 changed based on NMA nmodes parm99
CA-CA-OS 70.5 115.46 gaff, ce-c2-os forceconst, gaussian O-out
OS-CA-CA 70.5 115.46 gaff, ce-c2-os forceconst, gaussian O-out

DIHE
N2-CA-N2-H 4 9.60 180.0 2.0 parm 99, X -CA-N2-X
CA-CA-N2-H 4 9.60 180.0 2.0 parm 99, X -CA-N2-X
N2-CA-CA-CA 4 0.789 327.000 -4.0 DB921
N2-CA-CA-CA 4 -3.118 0.000 -2.0 DB921
N2-CA-CA-CA 4 0.609 90.000 1.0 DB921
CA-CA-CA-CA 4 14.50 180.0 2.0 parm99, X -CA-CA-X
CA-CA-CA-HA 4 14.50 180.0 2.0 parm99, X -CA-CA-X
HA-CA-CA-HA 4 14.50 180.0 2.0 parm99, X -CA-CA-X
CA-CA-CA-CB 4 14.50 180.0 2.0 parm99, X -CA-CA-X
CB-CA-CA-HA 4 14.50 180.0 2.0 parm99, X -CA-CA-X
CA-CA-CB-CB 4 14.00 180.0 2.0 parm99, X -CA-CB-X
HA-CA-CB-NB 4 14.00 180.0 2.0 parm99, X -CA-CB-X
HA-CA-CB-CB 4 14.00 180.0 2.0 parm99, X -CA-CB-X
CA-CA-CB-NB 4 14.00 180.0 2.0 parm99, X -CA-CB-X
CB-CB-N*-CK 4 6.60 180.0 2.0 parm99, X -CB-N*-X
CB-CB-N*-CT 4 6.60 180.0 2.0 parm99, X -CB-N*-X
CA-CB-N*-CT 4 6.60 180.0 2.0 parm99, X -CB-N*-X
CA-CB-CB-NB 4 21.80 180.0 2.0 parm99, X -CB-CB-X
CA-CB-CB-N* 4 21.80 180.0 2.0 parm99, X -CB-CB-X
CA-CB-NB-CK 2 5.10 180.0 2.0 parm99, X -CB-NB-X
N*-CK-NB-CB 2 20.00 180.0 2.0 parm99, X -CK-NB-X
C*-CK-NB-CB 2 20.00 180.0 2.0 parm99, X -CK-NB-X
NB-CK-N*-CB 4 6.80 180.0 2.0 parm99, X -CK-N*-X
C*-CK-N*-CB 4 6.80 180.0 2.0 parm99, X -CK-N*-X
C*-CK-N*-CT 4 6.80 180.0 2.0 parm99, X -CK-N*-X

N*-CK-C*-C* 4 3.42 180.0 2.0 New parameter for N*-CK-CA-CA
NB-CK-C*-C* 4 -0.6 180.0 -4.0 DB921 for NB-CK-CA-CA
NB-CK-C*-C* 4 3.1 180.0 -2.0 DB921 for NB-CK-CA-CA
NB-CK-C*-C* 4 -0.7 360.0 1.0 DB921 for NB-CK-CA-CA
HA-CA-CA-C* 4 14.50 180.0 2.0 parm99, X -CA-CA-X
CA-CA-CA-C* 4 14.50 180.0 2.0 parm99, X -CA-CA-X
CA-CA-C*-C* 4 -0.6 180.0 -4.0 DB921 for NB-CK-CA-CA
CA-CA-C*-C* 4 3.1 180.0 -2.0 DB921 for NB-CK-CA-CA
CA-CA-C*-C* 4 -0.7 360.0 1.0 DB921 for NB-CK-CA-CA
CA-CA-C*-S 4 3.42 180.0 2.0 New parameter for N*-CK-CA-CA
CA-C*-C*-HA 4 16.000 180.000 2.0 statistic value of parm94 X -cc-cc-X
HA-C*-C*-C* 4 16.000 180.000 2.0 statistic value of parm94 X -cc-cc-X
S -C*-C*-HA 4 16.000 180.000 2.0 statistic value of parm94 X -cc-cc-X
S -C*-C*-C* 4 16.000 180.000 2.0 statistic value of parm94 X -cc-cc-X
C*-C*-C*-HA 4 16.000 180.000 2.0 statistic value of parm94 X -cc-cc-X
C*-C*-C*-C* 4 16.000 180.000 2.0 statistic value of parm94 X -cc-cc-X
CA-C*-C*-C* 4 16.000 180.000 2.0 statistic value of parm94 X -cc-cc-X
HA-C*-C*-HA 4 16.000 180.000 2.0 statistic value of parm94 X -cc-cc-X
HA-C*-C*-CK 4 16.000 180.000 2.0 statistic value of parm94 X -cc-cc-X
CK-C*-C*-S 4 16.000 180.000 2.0 statistic value of parm94 X -cc-cc-X
C*-C*-C*-CK 4 16.000 180.000 2.0 statistic value of parm94 X -cc-cc-X
NB-CK-C*-S 4 -0.6 180.0 -4.0 DB921 for NB-CK-CA-CA
NB-CK-C*-S 4 3.1 180.0 -2.0 DB921 for NB-CK-CA-CA
NB-CK-C*-S 4 -0.7 360.0 1.0 DB921 for NB-CK-CA-CA
N*-CK-C*-S 4 -0.6 180.0 -4.0 DB921 for NB-CK-CA-CA
N*-CK-C*-S 4 3.1 180.0 -2.0 DB921 for NB-CK-CA-CA
N*-CK-C*-S 4 -0.7 360.0 1.0 DB921 for NB-CK-CA-CA
CA-C*-S -C* 2 2.200 180.000 2.0 X -c2-ss-X
H1-CT-N*-CK 1 0.00 000.0 -2. parm98, TC,PC,PAK FOR OS-CT-N*-CK
H1-CT-N*-CK 1 2.50 0.0 1. parm98, TC,PC,PAK FOR OS-CT-N*-CK
H1-CT-N*-CB 1 0.00 000.0 -2. parm98, TC,PC,PAK FOR OS-CT-N*-CK
H1-CT-N*-CB 1 2.50 0.0 1. parm98, TC,PC,PAK FOR OS-CT-N*-CK
CA-C*-S -C* 1 1.100 180.000 2.000 same as X -c2-ss-X, ca-cc-ss-cc generated by amber
C*-S -C*-C* 1 1.100 180.000 2.000 same as X -c2-ss-X, cc-ss-cc-cd generated by amber
C*-S -C*-CK 1 1.100 180.000 2.000 same as X -c2-ss-X, cc-ss-cc-cc generated by amber
OS-CA-CA-CA 4 14.50 180.0 2.0 parm99, X -CA-CA-X
OS-CA-CA-HA 4 14.50 180.0 2.0 parm99, X -CA-CA-X
CT-OS-CA-CA 2 3.29 180.000 2.000 New parameter
H1-CT-OS-CA 3 6.88 0.0 1.0 New parameter
CT-CT-OS-CA 3 6.88 0.0 1.0 New parameter
H1-CT-CT-OS 1 0.000 0.0 -3. JCC,7,(1986),230 PARM99
H1-CT-CT-OS 1 0.25 0.0 1. Junmei et al, 1999
H1-CT-CT-H1 1 0.15 0.0 3. Junmei et al, 1999 HC-CT-CT-HC PARM99
H1-CT-CT-CT 1 0.16 0.0 3. Junmei et al, 1999 HC-CT-CT-CT PARM99
CT-CT-CT-OS 9 1.40 0.0 3. JCC,7,(1986),230 X -CT-CT-X PARM99

IMPROPER
CA-CA-CA-C* 1.1 180.0 2.0 Using default value

CA-CA-CA-HA 1.1 180.0 2.0 General improper torsional angle (2 general atom types)
CA-CA-CA-CA 1.1 180.0 2.0 Using default value
CA-N2-CA-N2 1.1 180.0 2.0 Using default value
CA-C*-C*-S 1.1 180.0 2.0 Using default value
C*-C*-C*-HA 1.1 180.0 2.0 Using default value
C*-C*-C*-S 1.1 180.0 2.0 Using default value
CK-N*-CK-NB 1.1 180.0 2.0 Using default value
CA-CB-CB-NB 1.1 180.0 2.0 Using default value
CA-CB-CB-N* 1.1 180.0 2.0 Using default value
CA-CA-CA-HA 1.1 180.0 2.0 Using default value
CA-CA-CA-CA 1.1 180.0 2.0 Using default value
CA-N2-CA-N2 1.1 180.0 2.0 Using default value
CT-CK-N*-CB 1.1 180.0 2.0 Using default value

NONBON
H1 1.3870 0.0157 parm99
H 0.6000 0.0157 parm99
HA 1.4590 0.0150 parm99
CT 1.9080 0.1094 parm99
CA 1.9080 0.0860 parm99 (C*)
CB 1.9080 0.0860 parm99 (C*)
CK 1.9080 0.0860 parm99 (C*)
N* 1.8240 0.1700 parm99 (N)
NB 1.8240 0.1700 parm99 (N)
N2 1.8240 0.1700 parm99 (N)
C* 1.9080 0.0860 parm99
S 2.0000 0.2500 parm99
OS 1.6837 0.1700 parm99

NMR spectra of Key Intermediates and Final Products

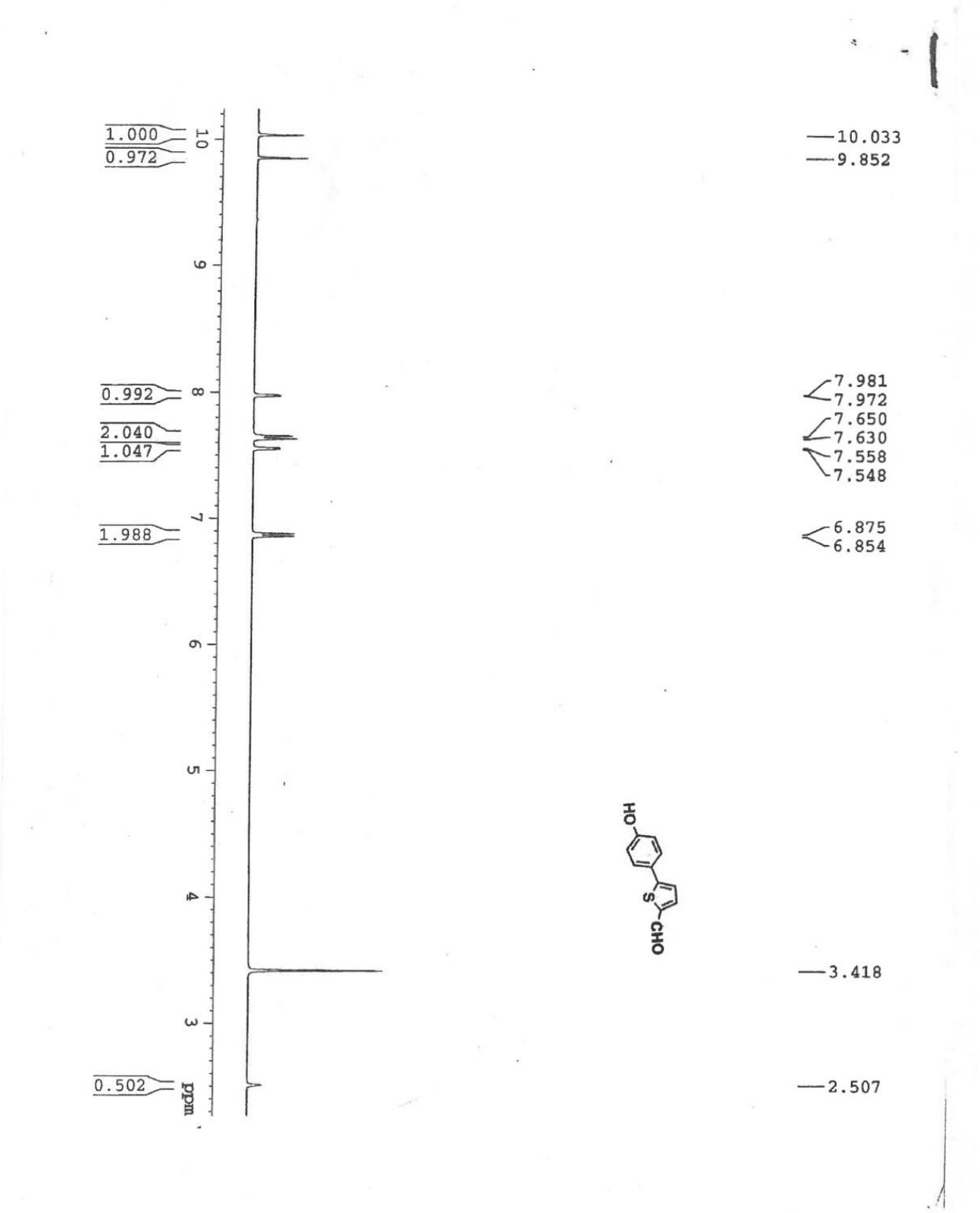

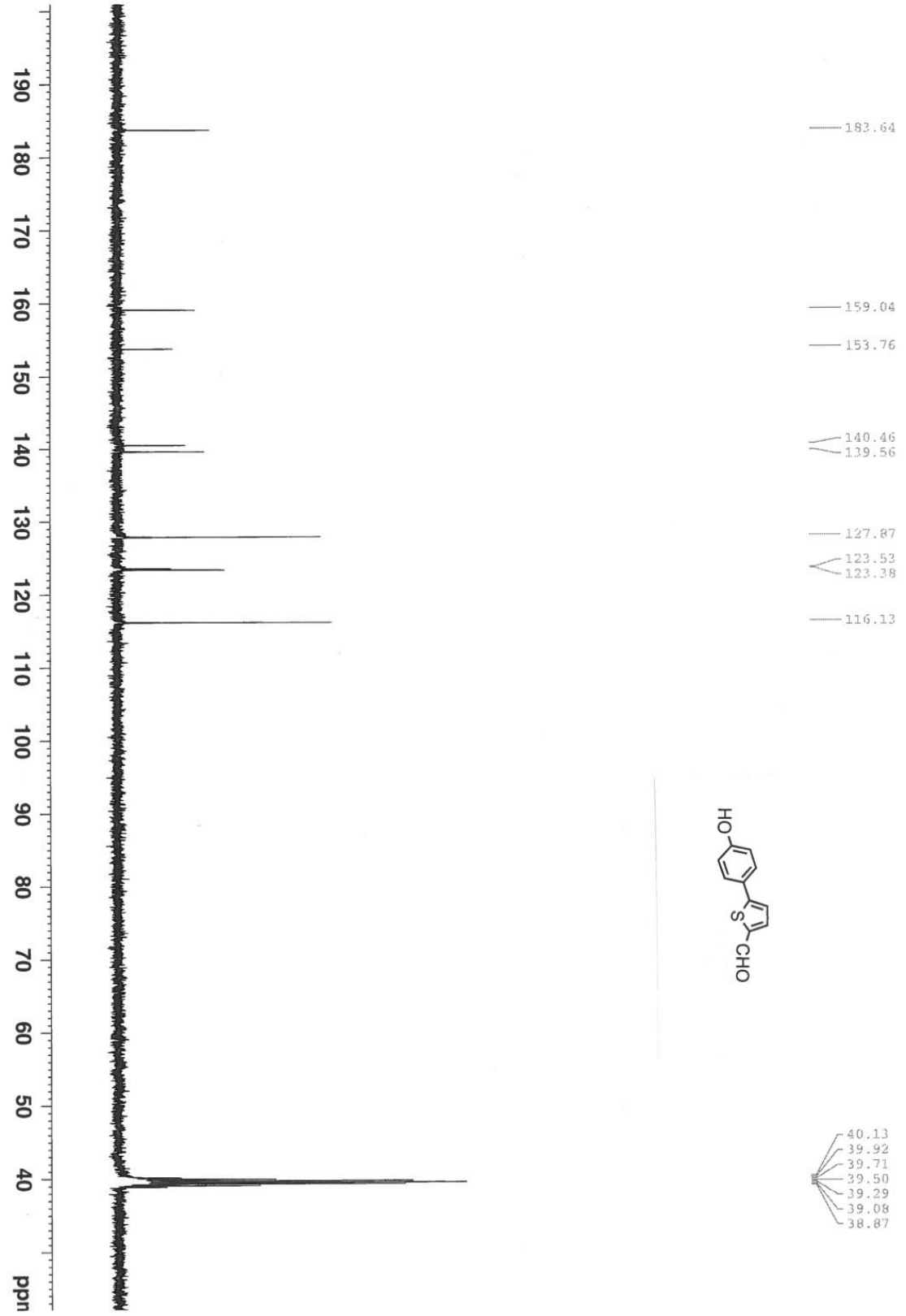
190
180
170
160
150
140
130
120
110
100
90
80
70
60
50
40
ppm
183.64
159.04
153.76
140.46
139.56
127.87
123.53
123.38
116.13
HO
S
CHO
40.13
39.92
39.71
39.50
39.29
39.08
38.87

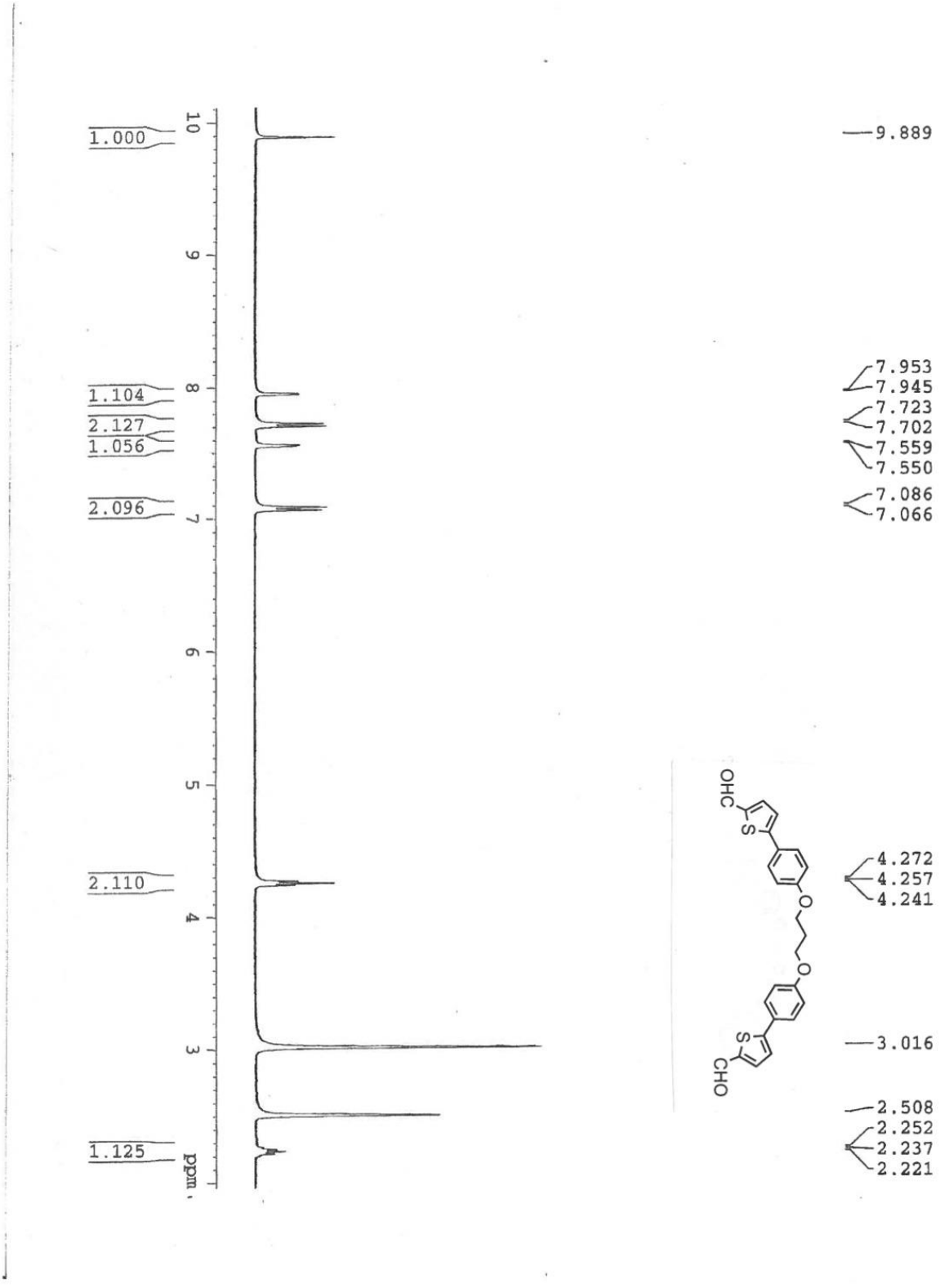
1.000
1.104
2.127
1.056
2.096
2.110
1.125
10
9
8
7
6
5
4
3
ppm
9.889
7.953
7.945
7.723
7.702
7.559
7.550
7.086
7.066
4.272
4.257
4.241
3.016
2.508
2.252
2.237
2.221
OHC
S
O
O
S
CHO

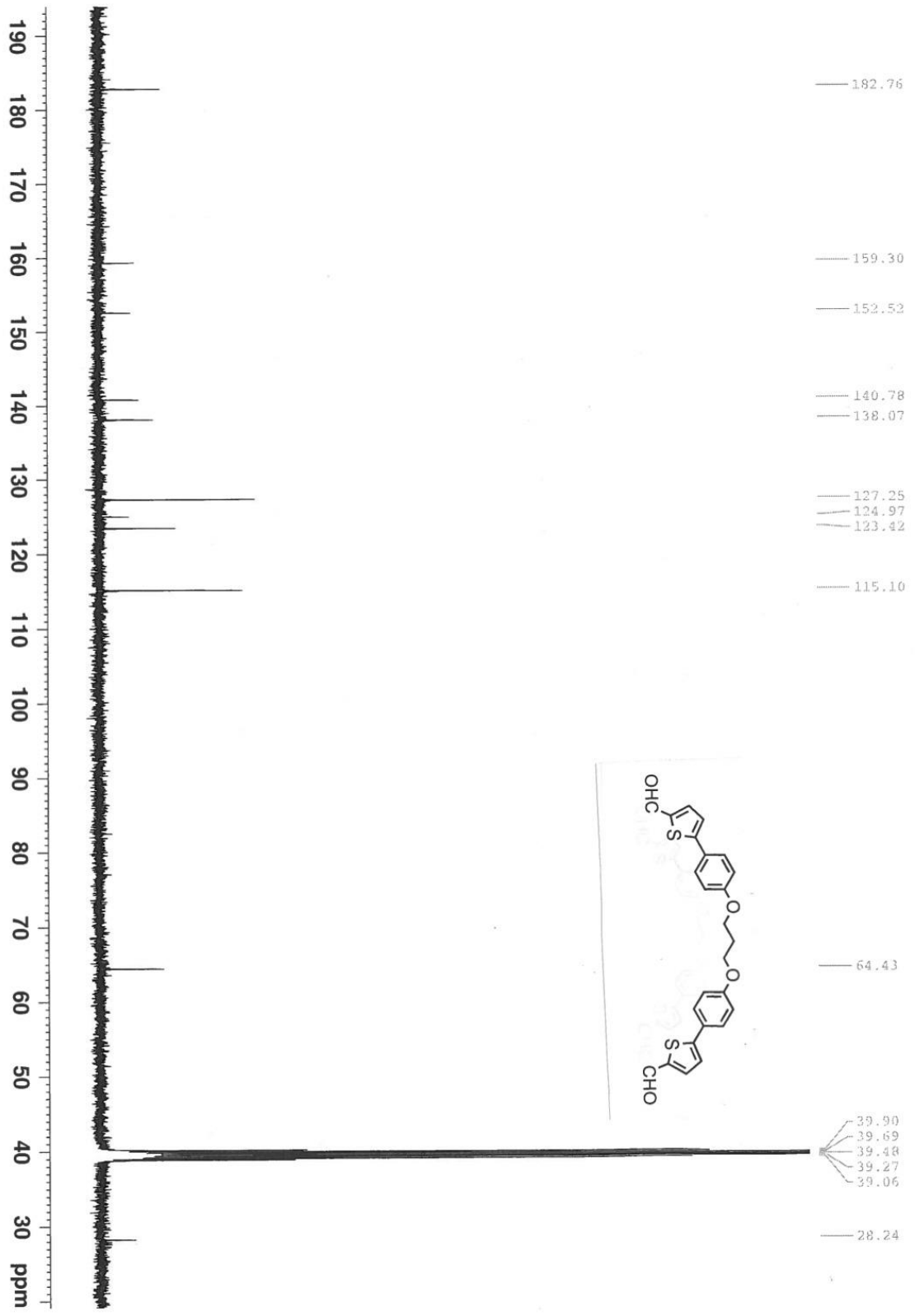
190
180
170
160
150
140
130
120
110
100
90
80
70
60
50
40
30
ppm
182.76
159.30
152.52
140.78
138.07
127.25
124.97
123.42
115.10
64.43
39.90
39.69
39.48
39.27
39.06
28.24
OHC
S
O
O
S
CHO

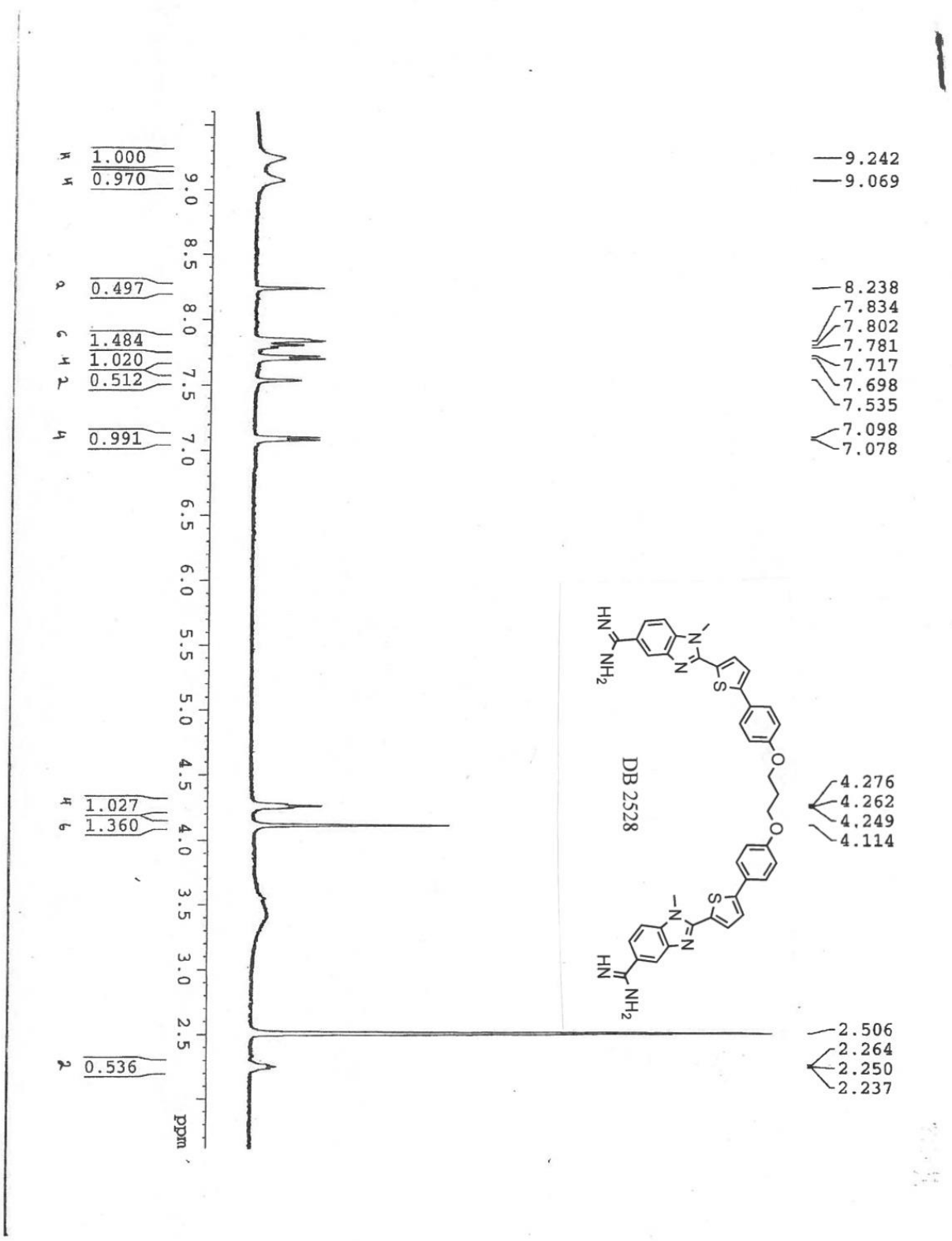
9.242
9.069
8.238
7.834
7.802
7.781
7.717
7.698
7.535
7.098
7.078
4.276
4.262
4.249
4.114
2.506
2.264
2.250
2.237
DB 2528
1.000
0.970
0.497
1.484
1.020
0.512
0.991
1.027
1.360
0.536
ppm

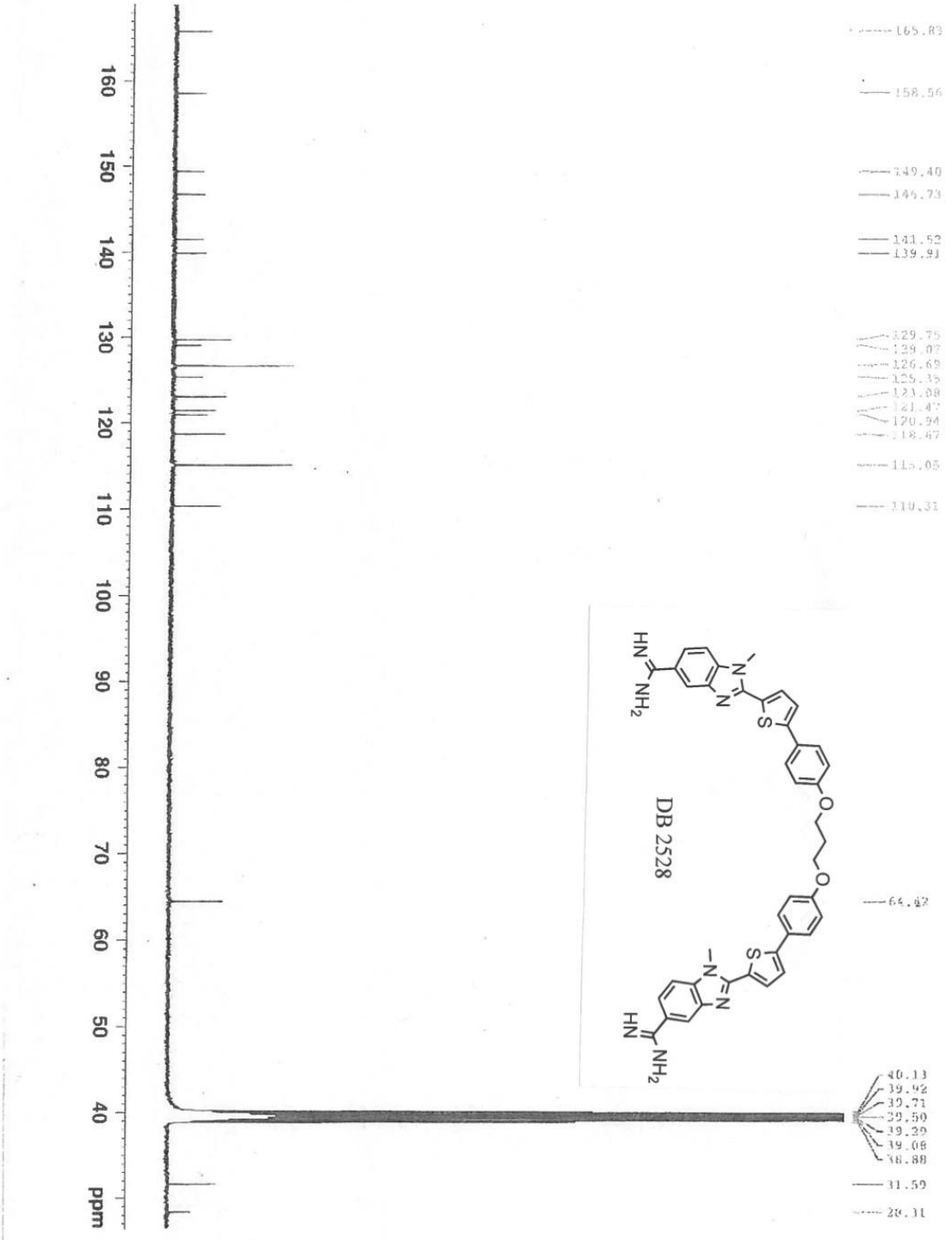
DB 2528
HN
NH2
N
S
O
ppm
160
150
140
130
120
110
100
90
80
70
60
50
40

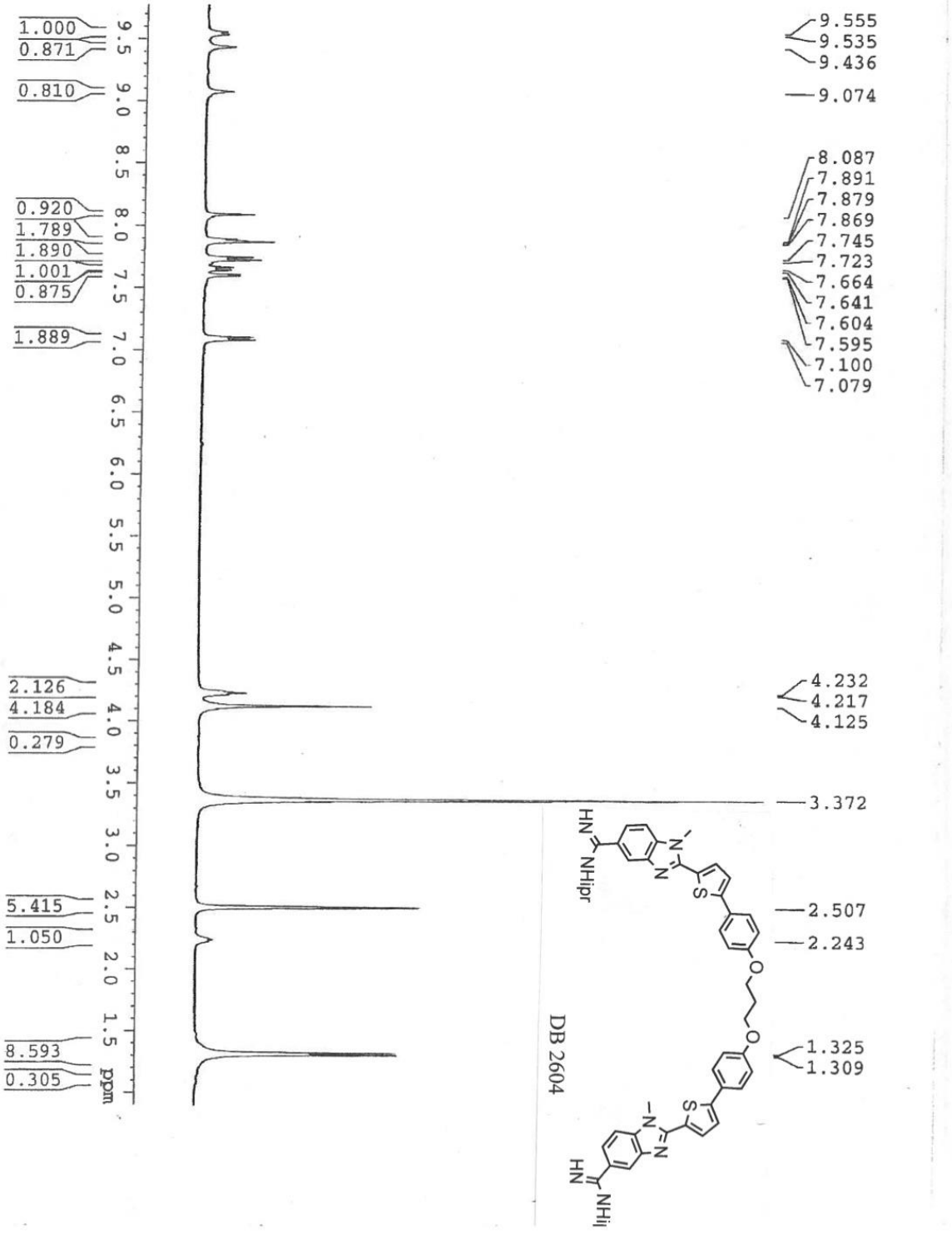
9.555
9.535
9.436
9.074
8.087
7.891
7.879
7.869
7.745
7.723
7.664
7.641
7.604
7.595
7.100
7.079
4.232
4.217
4.125
3.372
2.507
2.243
1.325
1.309
1.000
0.871
0.810
0.920
1.789
1.890
1.001
0.875
1.889
2.126
4.184
0.279
5.415
1.050
8.593
0.305
9.5 9.0 8.5 8.0 7.5 7.0 6.5 6.0 5.5 5.0 4.5 4.0 3.5 3.0 2.5 2.0 1.5 ppm
HN
NHipr
DB 2604

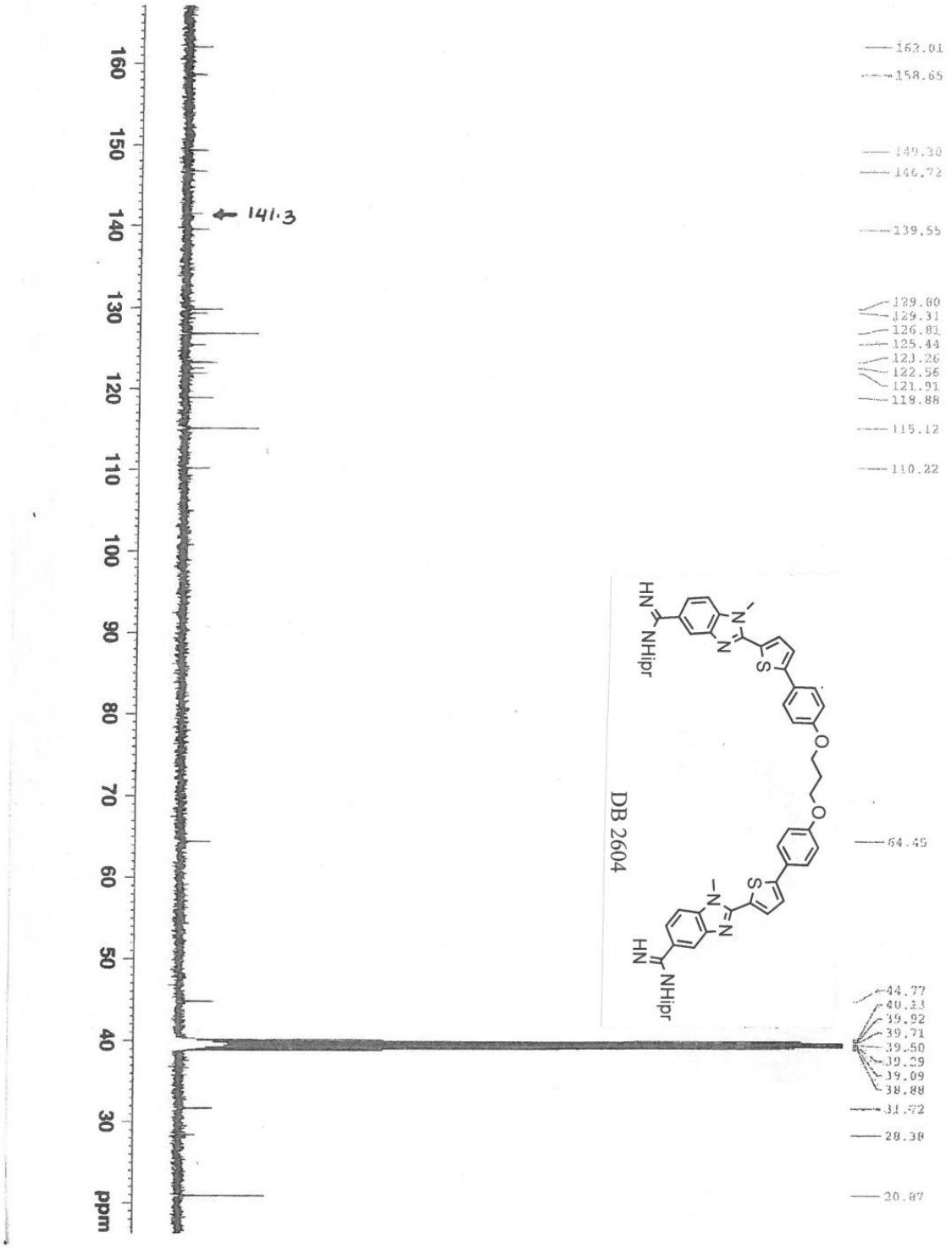
162.01
158.65
149.30
146.72
139.55
129.80
129.31
126.81
125.44
123.26
122.56
121.91
118.88
115.12
110.22
64.45
44.77
40.13
39.92
39.71
39.50
39.29
39.09
38.88
31.72
20.30
20.07
141.3
160
150
140
130
120
110
100
90
80
70
60
50
40
30
ppm
HN
NHipr
DB 2604

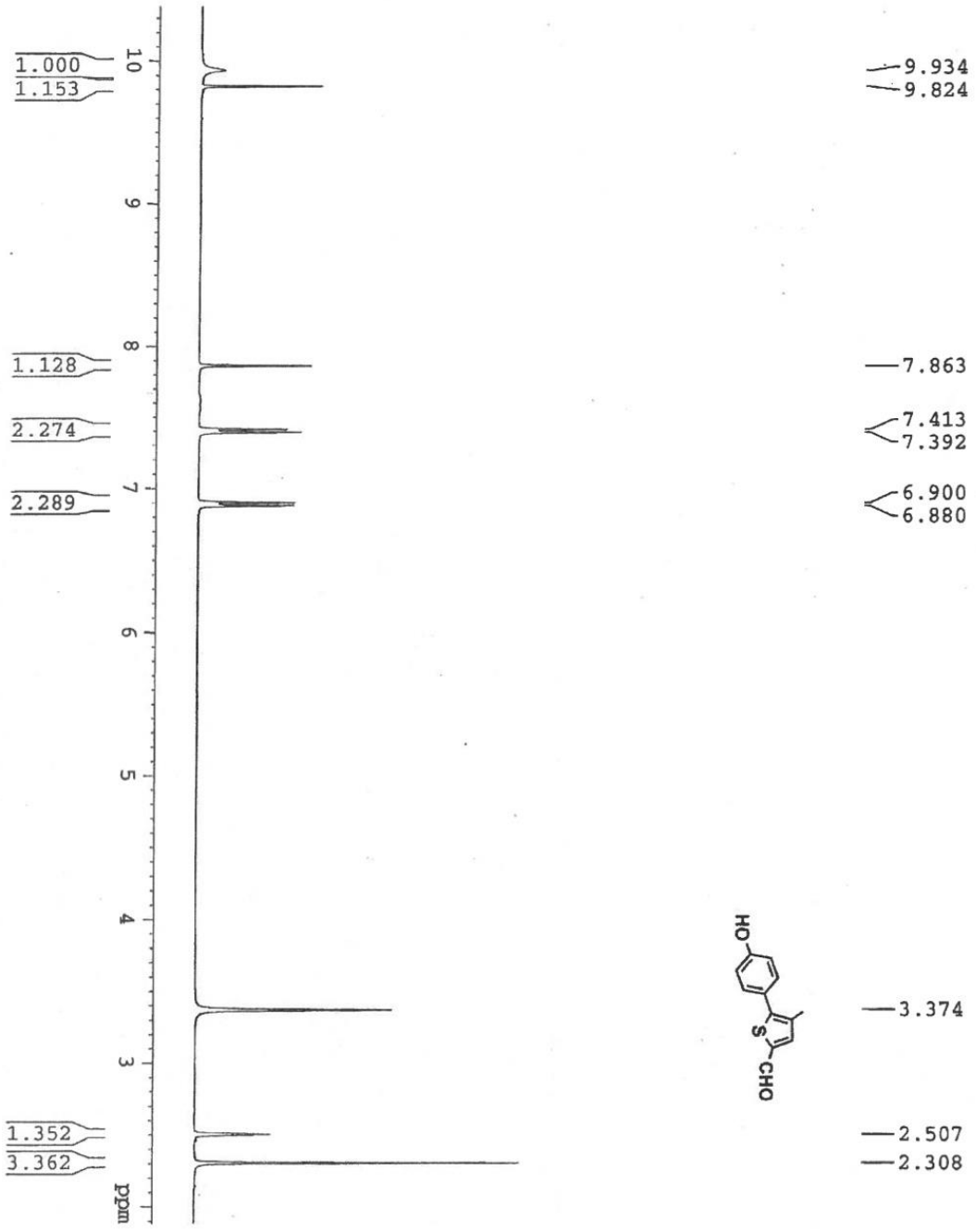
1.000
1.153
1.128
2.274
2.289
1.352
3.362
10
9
8
7
6
5
4
3
ppm
9.934
9.824
7.863
7.413
7.392
6.900
6.880
3.374
2.507
2.308
HO
S
CHO

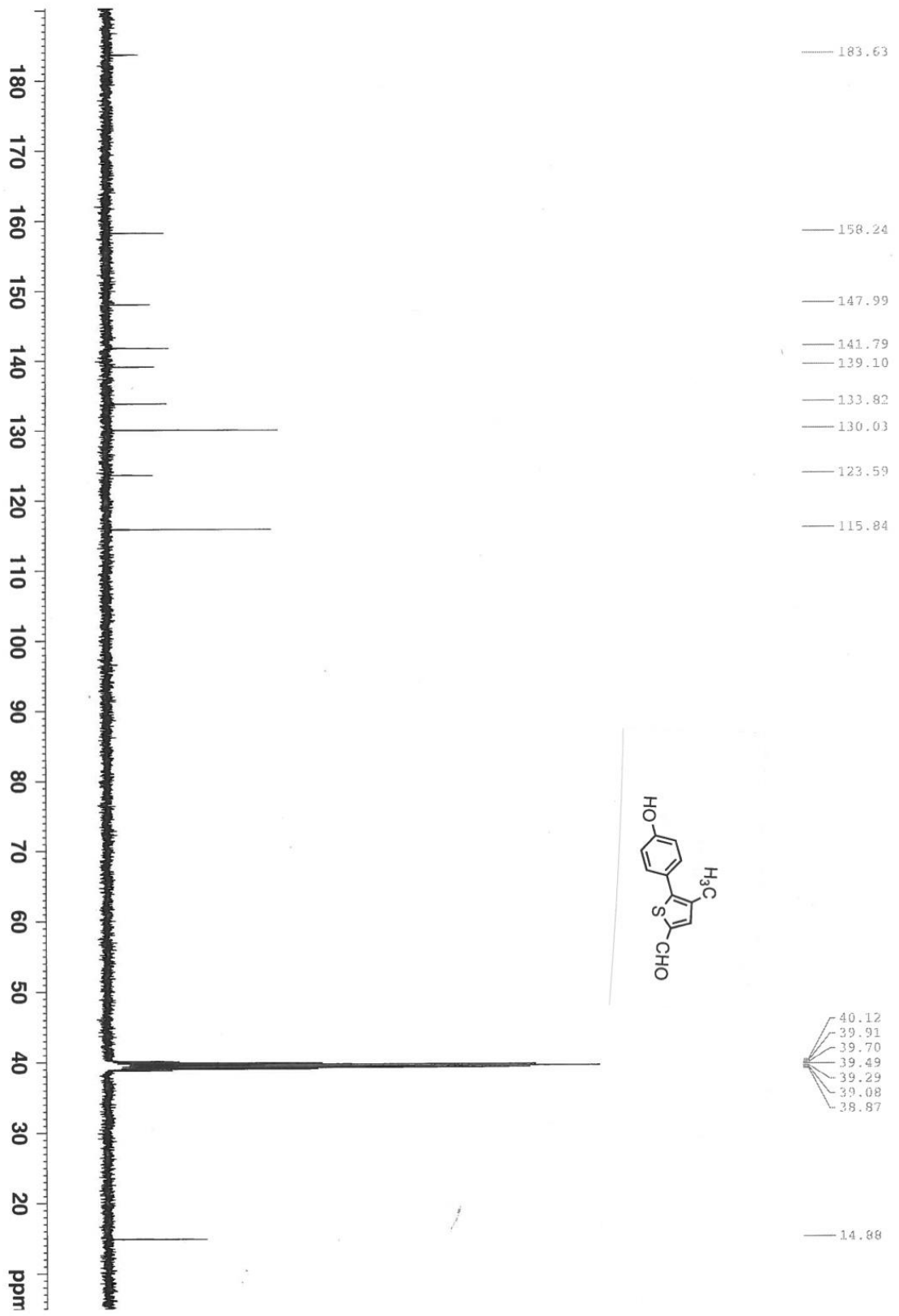
183.63
158.24
147.99
141.79
139.10
133.82
130.03
123.59
115.84
40.12
39.91
39.70
39.49
39.29
39.08
38.87
14.88
HO
H3C
S
CHO
180
170
160
150
140
130
120
110
100
90
80
70
60
50
40
30
20
ppm

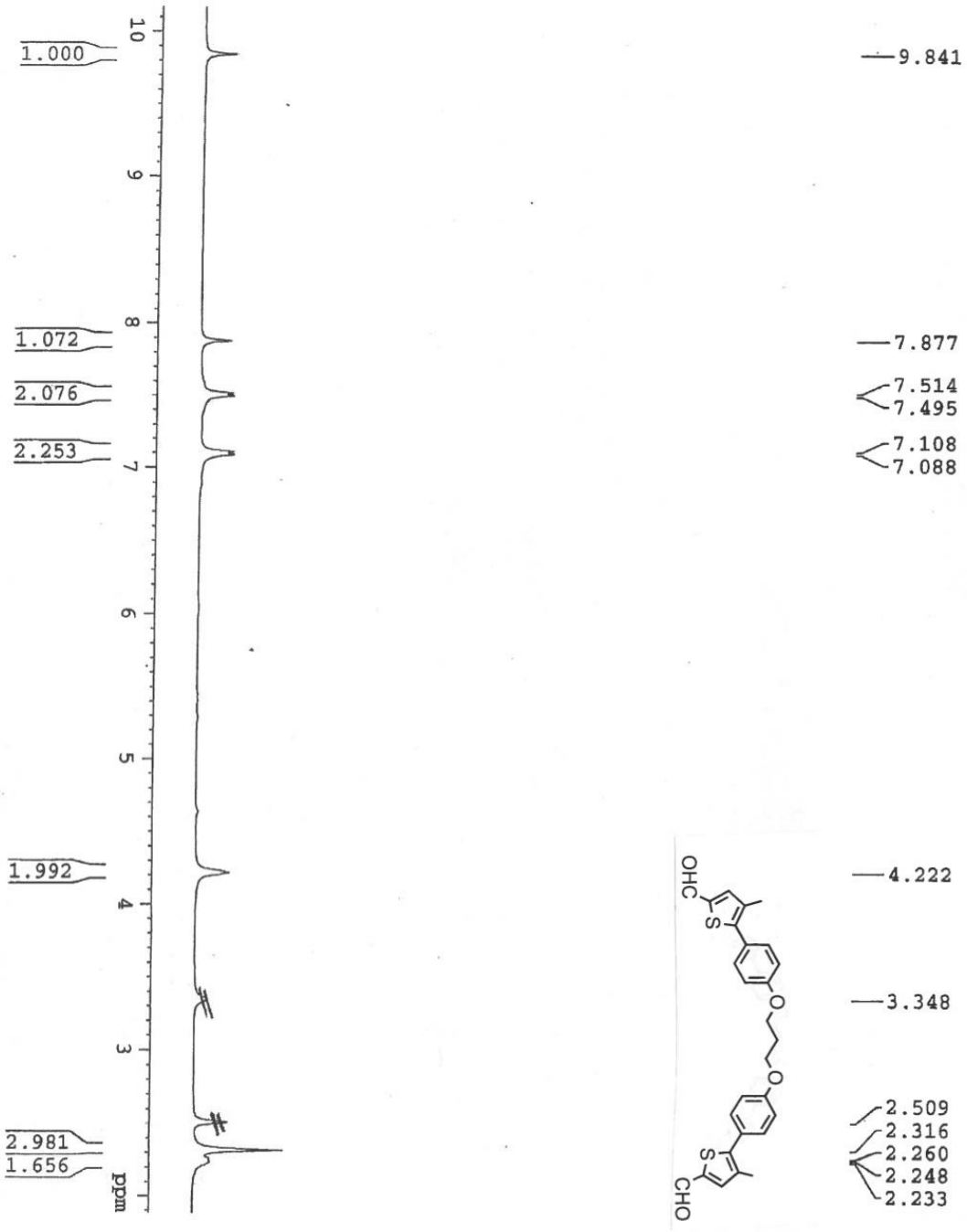
1.000
1.072
2.076
2.253
1.992
2.981
1.656
ppm
10
9
8
7
6
5
4
3
2
1
9.841
7.877
7.514
7.495
7.108
7.088
4.222
3.348
2.509
2.316
2.260
2.248
2.233
OHC
S
O
O
S
CHO

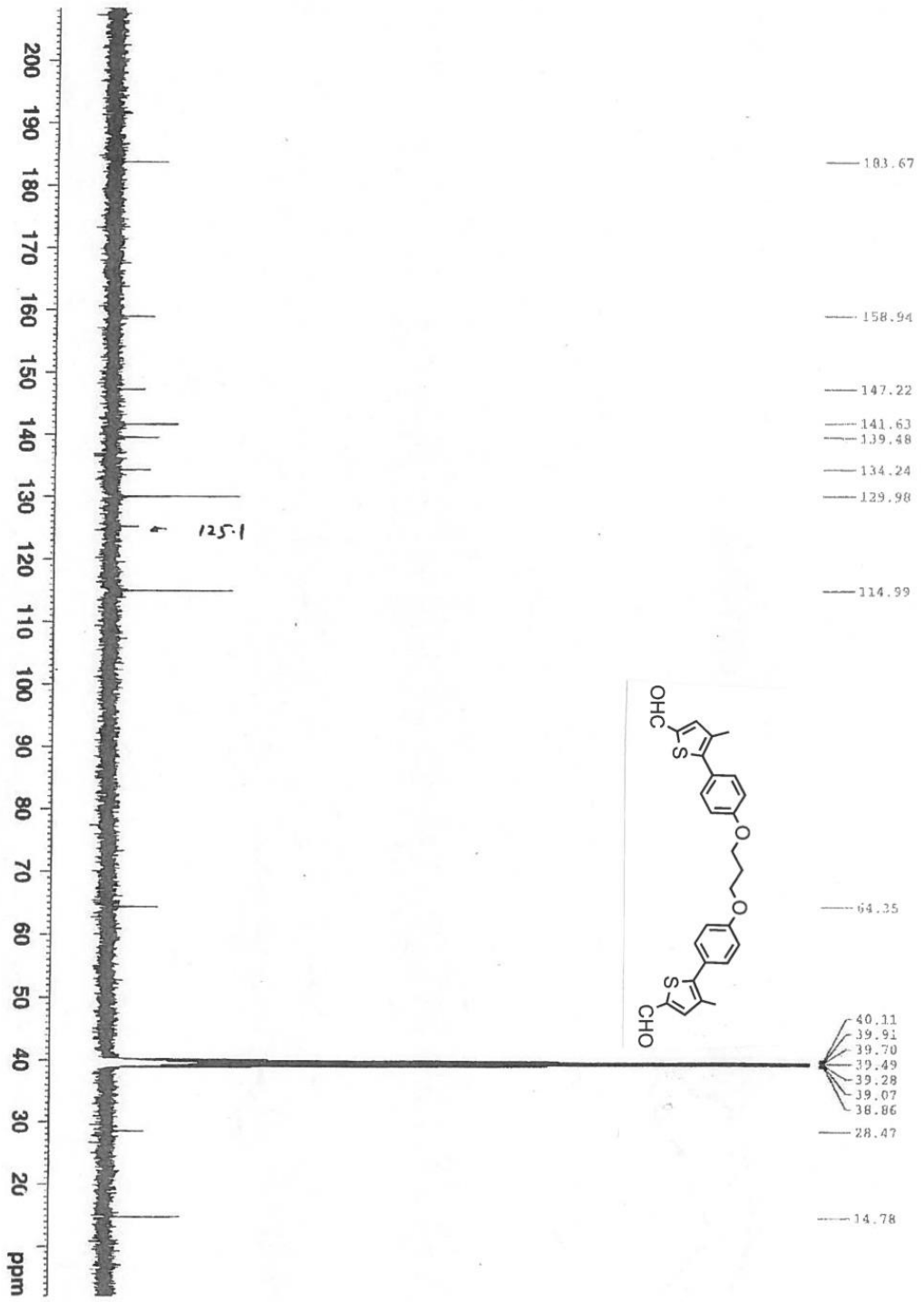
183.67
158.94
147.22
141.63
139.48
134.24
129.98
125.1
114.99
64.35
40.11
39.91
39.70
39.49
39.28
39.07
38.86
28.47
14.78
OHC
S
O
O
S
CHO
200 190 180 170 160 150 140 130 120 110 100 90 80 70 60 50 40 30 20
ppm

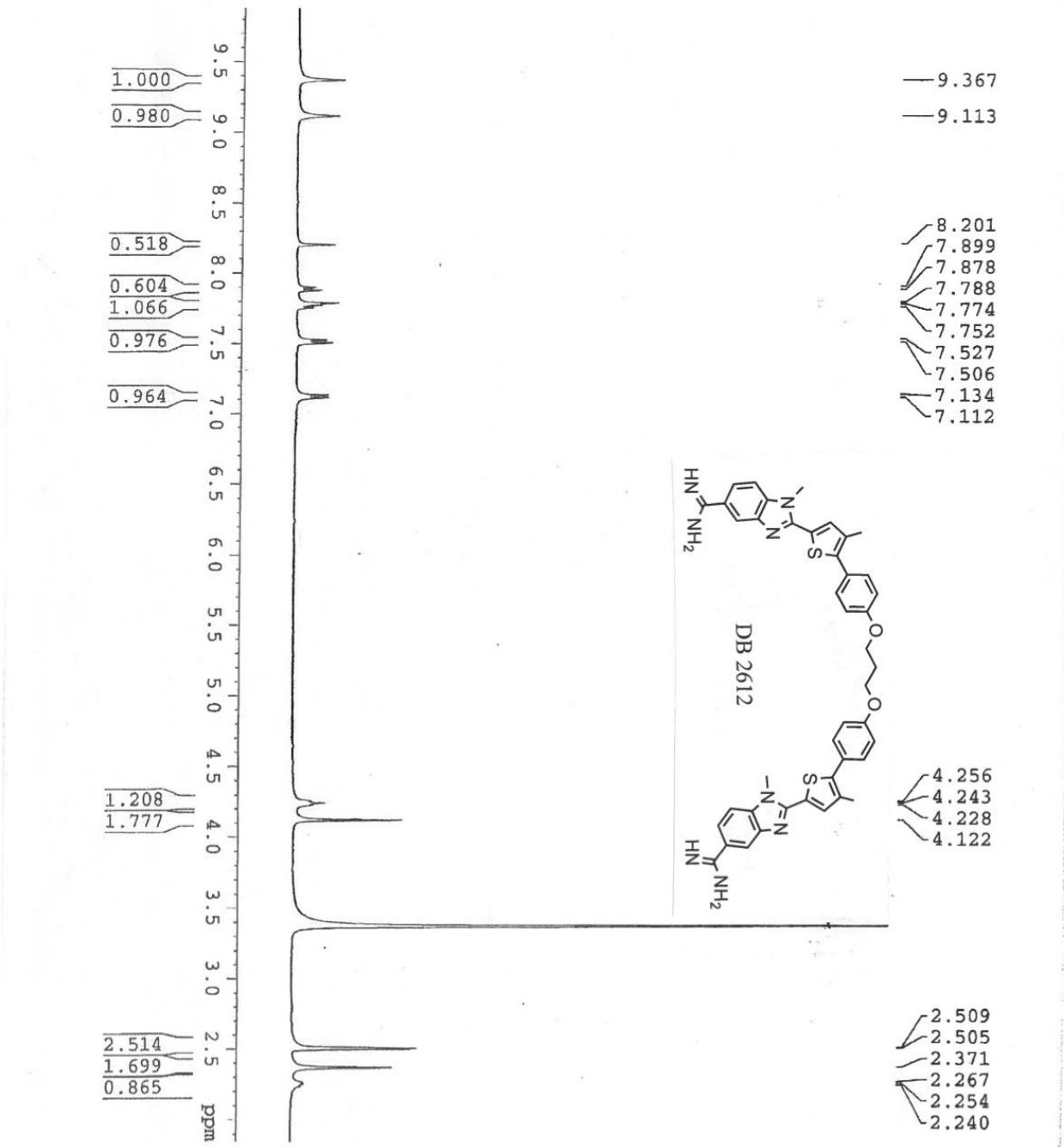
9.367
9.113
8.201
7.899
7.878
7.788
7.774
7.752
7.527
7.506
7.134
7.112
4.256
4.243
4.228
4.122
2.509
2.505
2.371
2.267
2.254
2.240
1.000
0.980
0.518
0.604
1.066
0.976
0.964
1.208
1.777
2.514
1.699
0.865
9.5 9.0 8.5 8.0 7.5 7.0 6.5 6.0 5.5 5.0 4.5 4.0 3.5 3.0 2.5 ppm
DB 2612

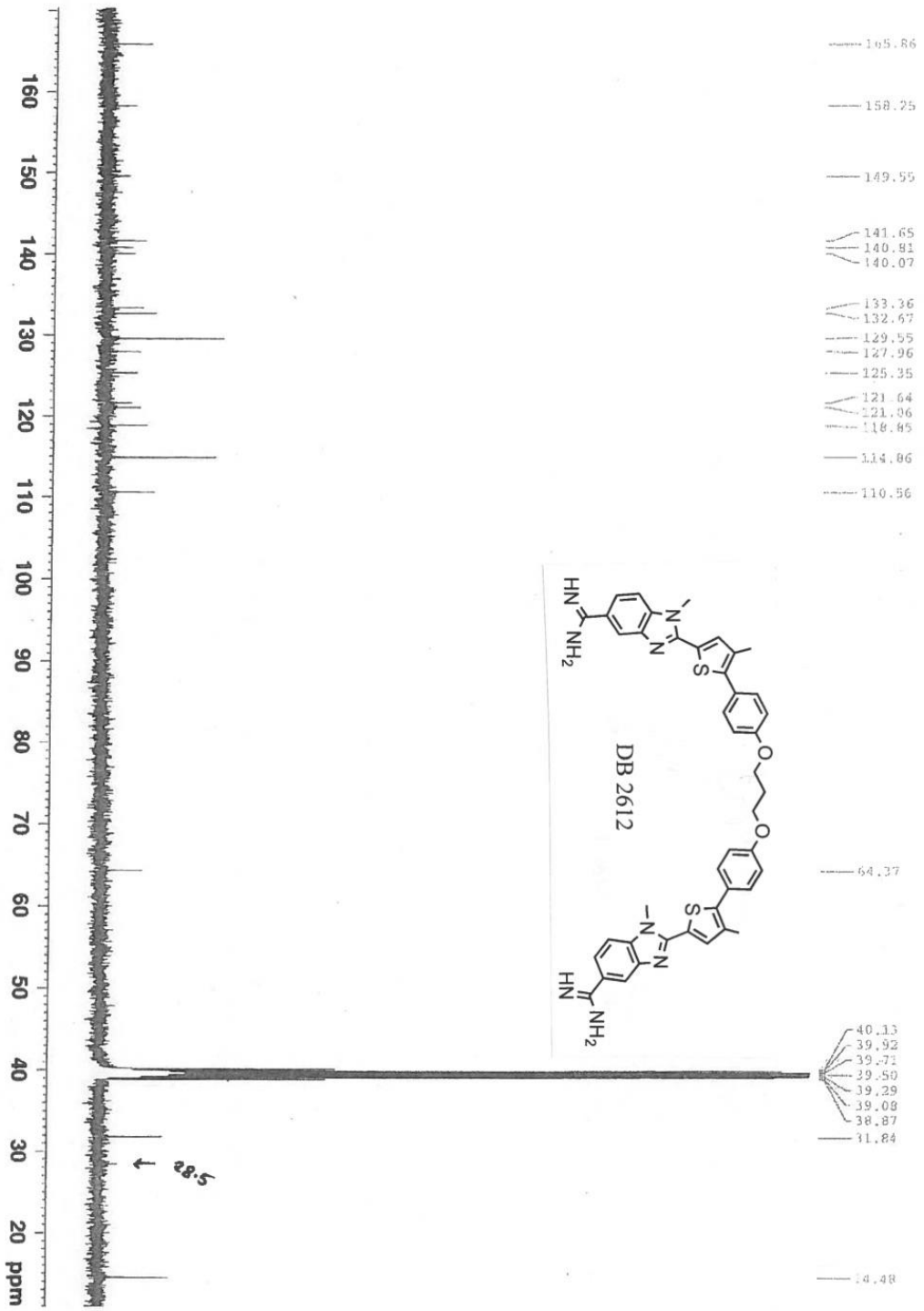
165.86
158.25
149.55
141.65
140.81
140.07
133.36
132.67
129.55
127.96
125.35
121.64
121.06
118.85
114.86
110.56
64.37
40.13
39.92
39.71
39.50
39.29
39.08
38.87
31.84
14.48
28.5
160
150
140
130
120
110
100
90
80
70
60
50
40
30
20 ppm
DB 2612
HN
NH2
N
S
O

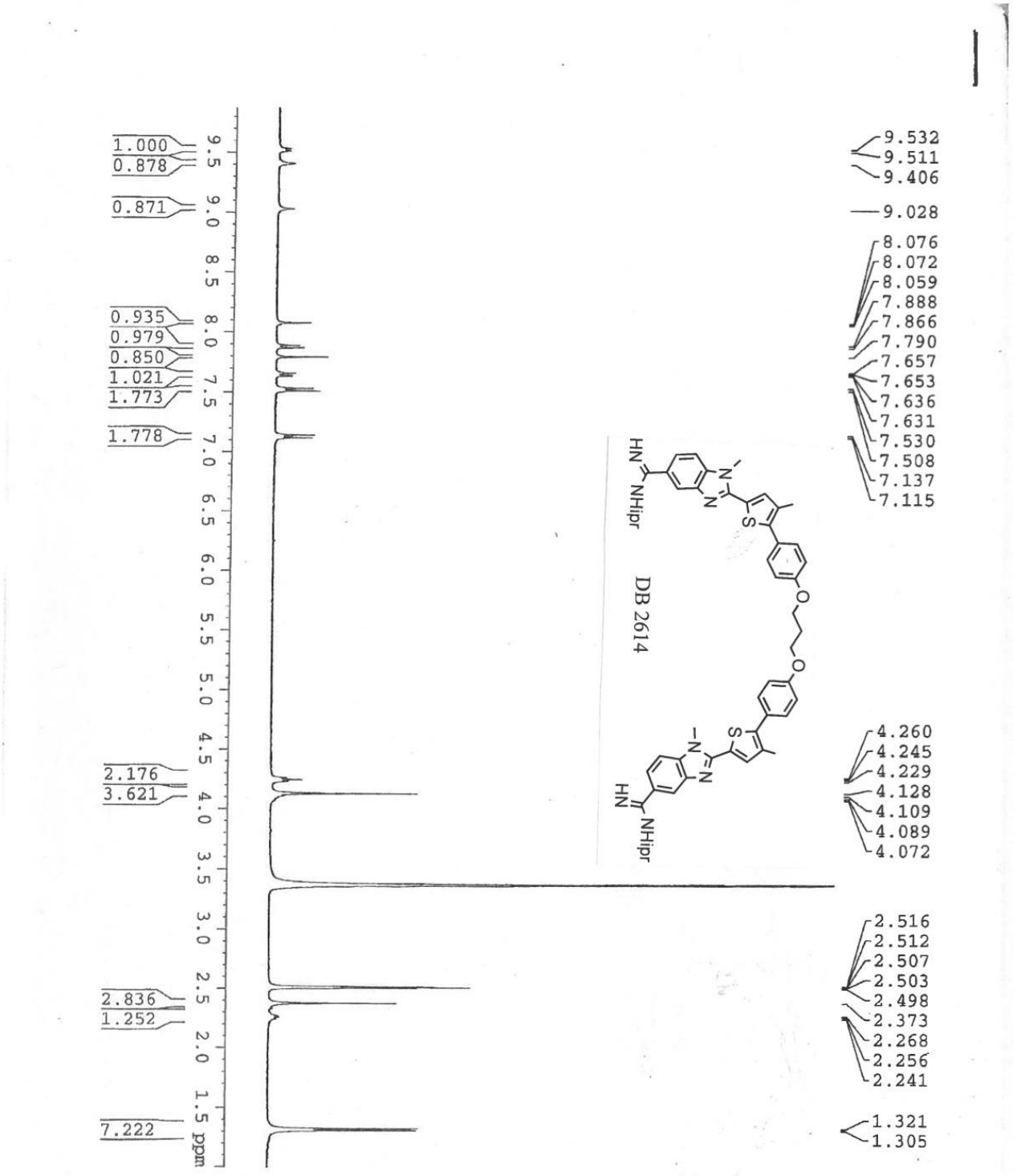
DB 2614
HN
NHipr
HN
NHipr
9.532
9.511
9.406
9.028
8.076
8.072
8.059
7.888
7.866
7.790
7.657
7.653
7.636
7.631
7.530
7.508
7.137
7.115
4.260
4.245
4.229
4.128
4.109
4.089
4.072
2.516
2.512
2.507
2.503
2.498
2.373
2.268
2.256
2.241
1.321
1.305
1.000
0.878
0.871
0.935
0.979
0.850
1.021
1.773
1.778
2.176
3.621
2.836
1.252
7.222
9.5
9.0
8.5
8.0
7.5
7.0
6.5
6.0
5.5
5.0
4.5
4.0
3.5
3.0
2.5
2.0
1.5
ppm

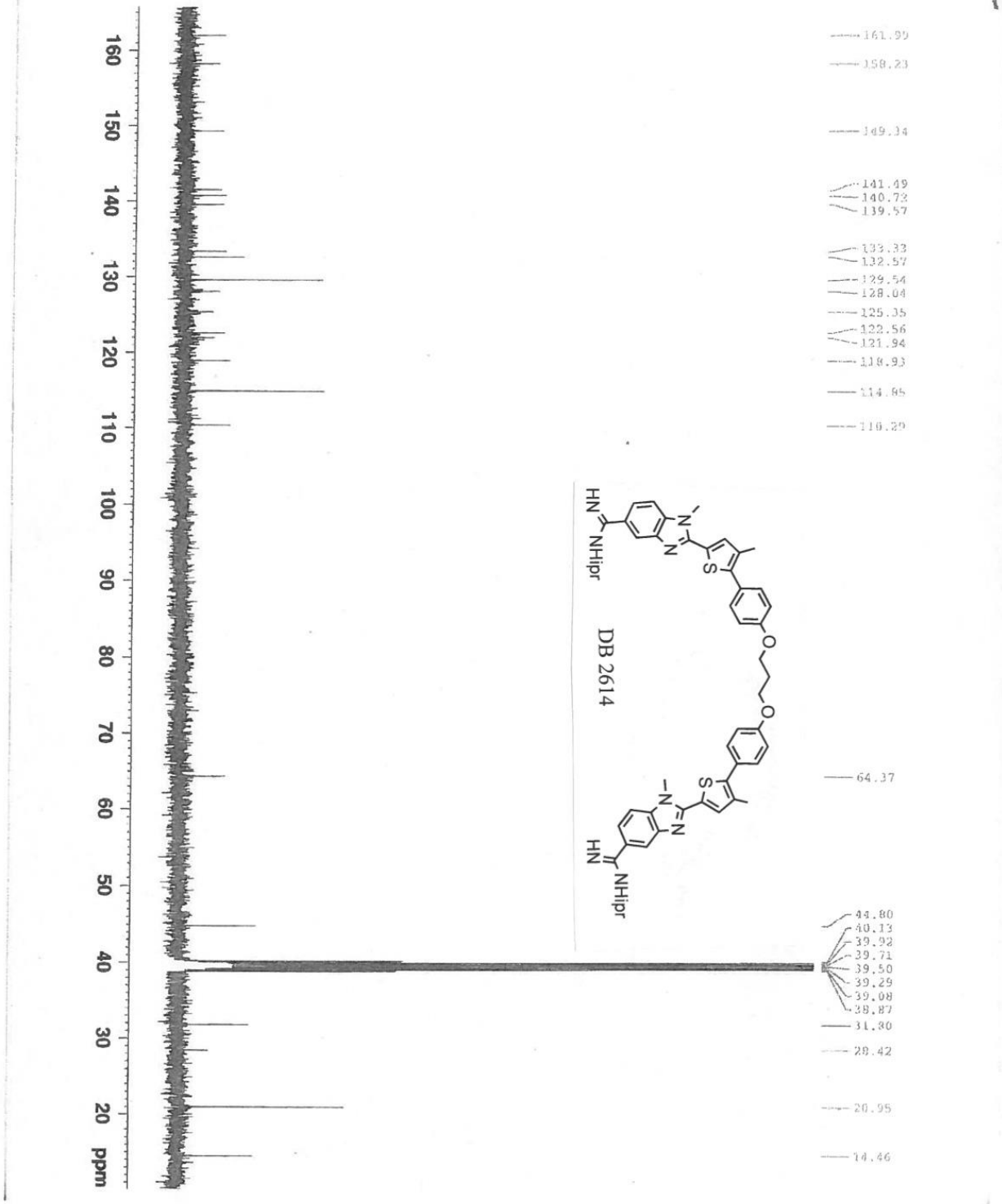
161.99
158.23
149.34
141.49
140.73
139.57
133.33
132.57
129.54
128.04
125.35
122.56
121.94
118.93
114.85
110.29
64.37
44.80
40.13
39.92
39.71
39.50
39.29
39.08
38.87
31.30
28.42
20.95
14.46
160
150
140
130
120
110
100
90
80
70
60
50
40
30
20
ppm
HN
NHipr
DB 2614
HN
NHipr

References

1 R. Nanjunda, M. Munde, Y. Liu, W. Wilson, in (Ed.: Y. Wanunu), Methods for Studying Nucleic Acid/Drug Interactions, **2011**, pp. 92–122.

2 Y. Liu, A. Kumar, S. Depauw, R. Nhili, M.-H. David-Cordonnier, M. P. Lee, M. A. Ismail, A. A. Farahat, M. Say, S. Chackal-Catoen, et al., *J. Am. Chem. Soc.* **2011**, *133*, 10171–10183.

3 M. Munde, A. Kumar, R. Nhili, S. Depauw, M.-H. David-Cordonnier, M. A. Ismail, C. E. Stephens, A. A. Farahat, A. Batista-Parra, D. W. Boykin, et al., *J. Mol. Biol.* **2010**, *402*, 847–864.

4 W. A. Lea, A. Simeonov, *Expert Opinion on Drug Discovery* **2010**, *6*, 17–32.

5 A. G. Kozlov, R. Galletto, T. M. Lohman, in *Single-Stranded DNA Binding Proteins*, Humana Press, Totowa, NJ, **2012**, pp. 55–83.

6 M. J. Frisch, G. W. Trucks, H. B. Schlegel, G. E. Scuseria, *Gaussian 09, Revision B. 01. Gaussian 09, Revision B. 01. Wallingford CT: Gaussian*, **2009**.

7 C. I. Bayly, P. Cieplak, W. Cornell, *J. Phys. Chem.* **1993**, *97*, 10269–10280.

8 U. C. Singh, P. A. Kollman, *J. Comput. Chem.* **1984**, *5*, 129–145.

9 D. A. Case, V. Babin, J. Berryman, R. M. Betz, Q. Cai, *Amber 14*, NYU Press, **2014**.

10 J. Wang, W. Wang, P. A. Kollman, D. A. Case, *J. Mol. Graph. Model.* **2006**, *25*, 247–260.

11 P. Athri, W. D. Wilson, *J. Am. Chem. Soc.* **2009**, *131*, 7618–7625.

12 N. Špačková, T. E. Cheatham, F. Ryjáček, F. Lankaš, L. van Meervelt, P. Hobza, J. Šponer, *J. Am. Chem. Soc.* **2003**, *125*, 1759–1769.

13 O. Trott, A. J. Olson, *J. Comput. Chem.* **2010**, *31*, 455–461.